Table 2. Differentially expressed proteins that characterize histological subtypes of epithelial ovarian carcinoma, screened by two-dimensional gel electrophoresis and identified by matrix-assisted laser desorption ionization time-of-flight mass spectrometry (proteins identified from multiple individual spots are indicated in parentheses and are numbered in order of abundance)

UniProt ID	Gene symbol	Protein name	*P*-value*	Fold change	Cellular component†
Clear cell carcinoma					
Upregulated					
P00491	*PNP*	Purine nucleoside phosphorylase (#1 of 4 spots)	1.3E-06	2.38	Cytoplasm
P60174	*TPI1*	Triosephosphate isomerase (#3 of 4)	7.6E-06	2.36	Cytoplasm, nucleus
P07942	*LAMB1*	Laminin subunit β-1	7.7E-06	4.71	Plasma membrane, extracellular space
P09525	*ANXA4*	Annexin A4 (#1 of 2)	1.4E-05	2.52	Cytoplasm
Q9Y617	*PSAT1*	Phosphoserine aminotransferase (#1 of 2)	2.4E-05	2.49	n/a
P09525	*ANXA4*	Annexin A4 (#2 of 2)	4.0E-05	3.97	Cytoplasm
P07195	*LDHB*	L-Lactate dehydrogenase B chain	4.0E-05	1.62	Cytoplasm, mitochondrion
P23381	*WARS*	Tryptophanyl-tRNA synthetase, cytoplasmic	5.6E-05	4.06	Cytoplasm
O00764	*PDXK*	Pyridoxal kinase	1.2E-04	1.91	Cytoplasm
P11047	*LAMC1*	Laminin subunit γ-1	1.4E-04	3.31	Extracellular space
Q9Y617	*PSAT1*	Phosphoserine aminotransferase (#2 of 2)	1.4E-04	4.06	n/a
Q16762	*TST*	Thiosulfate sulfurtransferase (#2 of 2)	1.4E-04	2.54	Mitochondrion, plasma membrane
P30040	*ERP29*	Endoplasmic reticulum resident protein 29	1.9E-04	1.86	Cytoplasm
Q8WW59	*SPRYD4*	SPRY domain-containing protein 4	1.9E-04	1.74	Mitochondrion, nucleus
P04179	*SOD2*	Superoxide dismutase (Mn), mitochondrial	2.2E-04	2.39	Cytoplasm, mitochondrion
P22352	*GPX3*	Glutathione peroxidase 3	3.4E-04	2.25	Extracellular space
P32119	*PRDX2*	Peroxiredoxin-2 (#2 of 3)	8.6E-04	2.35	Cytoplasm, mitochondrion
Q99536	*VAT1*	Synaptic vesicle membrane protein VAT-1 homolog	9.8E-04	1.76	Cytoplasm
Q13510	*ASAH1*	Acid ceramidase	0.0014	2.48	Cytoplasm
P02794	*FRIH*	Ferritin heavy chain	0.0016	1.57	Cytoplasm, mitochondrion
P40261	*NNMT*	Nicotinamide *N*-methyltransferase	0.0018	2.44	Cytoplasm
Q5EBM0	*CMPK2*	UMP-CMP kinase 2, mitochondrial	0.0031	2.14	Mitochondrion
O15305	*PMM2*	Phosphomannomutase 2	0.0035	1.42	Cytoplasm
P00491	*PNP*	Purine nucleoside phosphorylase (#4 of 4)	0.0035	2.42	Cytoplasm
P30041	*PRDX6*	Peroxiredoxin-6	0.0039	1.78	Cytoplasm, mitochondrion
Q9HCC0	*MCCC2*	Methylcrotonoyl-CoA carboxylase β chain, mitochondrial	0.0053	1.76	Mitochondrion
P02743	*SAMP*	Serum amyloid P-component	0.0071	1.98	Extracellular space
P21964	*COMT*	Catechol *O*-methyltransferase (#1 of 2)	0.0079	1.45	Cytoplasm, mitochondrion, plasma membrane
P30084	*ECHS1*	Enoyl-CoA hydratase, mitochondrial	0.0079	1.44	Mitochondrion
P00918	*CA2*	Carbonic anhydrase 2	0.0087	1.77	Cytoplasm, extracellular space
P04083	*ANXA1*	Annexin A1 (#2 of 3)	0.010	1.52	Cytoplasm, nucleus, plasma membrane, extracellular space
P24666	*ACP1*	Low molecular weight phosphotyrosine protein phosphatase (#2 of 3)	0.010	2.25	Cytoplasm, nucleus, plasma membrane
Q01105	*SET*	Protein SET	0.011	2.06	Cytoplasm, nucleus
P37837	*TALDO*	Transaldolase	0.011	1.80	Cytoplasm
Downregulated					
Q14019	*COTL*	Coactosin-like protein	4.0E-05	0.55	Cytoplasm
P06702	*S100A9*	Protein S100-A9 (#1 of 4)	9.1E-05	0.60	Cytoplasm, nucleus, plasma membrane, extracellular space
Q9P1F3	*C6ORF115*	Costars family protein C6orf115	3.0E-04	0.37	n/a
Q01469	*FABP5*	Fatty acid-binding protein, epidermal (#2 of 2)	5.9E-04	0.35	Cytoplasm
P29373	*CRABP2*	Cellular retinoic acid-binding protein 2	0.0028	0.24	Cytoplasm, nucleus
Q00169	*PITPNA*	Phosphatidylinositol transfer protein α isoform	0.0031	0.64	Cytoplasm
P07108	*DBI*	Acyl-CoA-binding protein	0.0048	0.60	n/a
P12429	*ANXA3*	Annexin A3	0.0053	0.59	Cytoplasm, plasma membrane
Q13228	*SELENBP1*	Selenium-binding protein 1	0.0059	0.62	Cytoplasm, nucleus
O95865	*DDAH2*	N^G,N^G-Dimethylarginine dimethylaminohydrolase 2	0.0071	0.63	Cytoplasm
P26447	*S100A4*	Protein S100-A4	0.0071	0.36	Cytoplasm, nucleus
P52907	*CAPZA1*	F-Actin capping protein subunit α-1	0.0079	0.72	Cytoplasm
P36952	*SPB5*	Serpin B5	0.0105	0.25	Cytoplasm, extracellular space
Endometrioid carcinoma					
Upregulated					
Q7L266	*ASRGL1*	L-Asparaginase	0.0046	3.59	Cytoplasm, nucleus
Q9P1F3	*C6ORF115*	Costars family protein C6orf115	0.0089	1.96	n/a

doi: 10.1111/j.1349-7006.2012.02224.x

Table 2. (continued)

UniProt ID	Gene symbol	Protein name	*P*-value*	Fold change	Cellular component†
Downregulated					
P09525	*ANXA4*	Annexin A4 (#2 of 2)	0.0007	0.21	Cytoplasm
O00299	*CLIC1*	Chloride intracellular channel protein 1 (#1 of 3)	0.0022	0.65	Cytoplasm, nucleus, plasma membrane
Q92597	*NDRG1*	Protein NDRG1	0.0032	0.52	Cytoplasm, nucleus, plasma membrane
P40925	*MDH1*	Malate dehydrogenase, cytoplasmic	0.0052	0.58	Cytoplasm, mitochondrion
P50583	*NUDT1*	Bis(5'-nucleosyl)-tetraphosphatase (asymmetrical)	0.0110	0.41	Mitochondrion
Mucinous carcinoma					
Upregulated					
P36952	*SPB5*	Serpin B5	1.0E-04	4.76	Cytoplasm, extracellular space
P18085	*ARF4*	ADP-ribosylation factor 4 (#2 of 2)	0.0016	2.93	Cytoplasm, plasma membrane
P37802	*TAGLN2*	Transgelin-2 (#1 of 2)	0.0045	3.62	Nucleus, plasma membrane
P12429	*ANXA3*	Annexin A3	0.0052	1.60	Cytoplasm, plasma membrane
Downregulated					
P32119	*PRDX2*	Peroxiredoxin-2 (#2 of 3)	0.0045	0.39	Cytoplasm, mitochondrion
Q13938	*CAPS*	Calcyphosin	0.0052	0.27	Cytoplasm
P02794	*FRIH*	Ferritin heavy chain	0.0061	0.53	Cytoplasm, mitochondrion
O00764	*PDXK*	Pyridoxal kinase	0.011	0.52	Cytoplasm
P24666	*ACP1*	Low molecular weight phosphotyrosine protein phosphatase (#1 of 2)	0.011	0.43	Cytoplasm, nucleus, plasma membrane
Serous carcinoma					
Upregulated					
P29373	*CRABP2*	Cellular retinoic acid-binding protein 2	9.4E-05	3.82	Cytoplasm, nucleus
O43598	*C6ORF108*	Deoxyribonucleoside 5'-monophosphate *N*-glycosidase	0.0010	2.21	Cytoplasm, nucleus
P24666	*ACP1*	Low molecular weight phosphotyrosine protein phosphatase (#1 of 2)	0.0010	1.68	Cytoplasm, nucleus, plasma membrane
P61769	*B2M*	β-2-Microglobulin	0.0029	1.68	Cytoplasm, plasma membrane, extracellular space
P00491	*PNP*	Purine nucleoside phosphorylase (#4 of 4)	0.0032	1.58	Cytoplasm
P42771	*CDKN2A*	Cyclin-dependent kinase inhibitor 2A, isoforms 1/2/3 (#3 of 3)	0.0037	3.35	Cytoplasm, nucleus
O95865	*DDAH2*	N^G,N^G-Dimethylarginine dimethylaminohydrolase 2	0.0046	1.59	Cytoplasm
P42771	*CDKN2A*	Cyclin-dependent kinase inhibitor 2A, isoforms 1/2/3 (#1 of 3)	0.0058	1.58	Cytoplasm, nucleus
P52907	*CAPZA1*	F-Actin capping protein subunit α-1	0.0080	2.36	Cytoplasm
P26447	*S100A4*	Protein S100-A4	0.0080	1.39	Cytoplasm, nucleus
P60174	*TPI1*	Triosephosphate isomerase (#4 of 4)	0.0110	1.33	Cytoplasm, nucleus
Downregulated					
P00491	*PNP*	Purine nucleoside phosphorylase (#1 of 4)	0.0022	0.51	Cytoplasm
Q13510	*ASAH1*	Acid ceramidase	0.0065	0.42	Cytoplasm
Q9HCC0	*MCCC2*	Methylcrotonoyl-CoA carboxylase β chain, mitochondrial	0.0080	0.53	Mitochondrion

n/a, no annotated terms; UMP-CMP, uridine monophosphate-cytidine monophosphate. **P*-values were calculated by the Mann–Whitney *U*-test. †The gene ontology (GO) terms searched for were: cytoplasm, mitochondrion, nucleus, plasma membrane and extracellular space.

and 4 of purine nucleoside phosphorylase were oppositely regulated in clear cell and serous carcinoma. For ANXA4 and PSAT1, all spots observed were concomitantly upregulated in clear cell carcinoma, reflecting the total change in protein expression.

Principal component analysis (PCA) was performed using the expression values of the 77 selected spots to visualize the expression pattern of 39 samples (Fig. 2b). The pattern clearly showed that clear cell carcinoma (rectangles in Fig. 2b) was most distinct from other subtypes, and that all samples of clear cell carcinoma were very homogeneous, with 11 samples forming a very confined cluster. The PCA plot also conveyed that clear cell and serous carcinomas were most distant, suggesting that the list of candidate biomarkers would perform best in distinguishing these two subtypes. Endometrioid samples exhibited remarkable overlap with other subtypes, conveying its expressional heterogeneity, concordant with the discovery of the smallest number of specifically up- or downregulated proteins for this subtype (two upregulated and five downregulated).

Validation by western blotting. The four proteins that exhibited the largest quantitative specificity to represent each subtype, namely ANXA4, PSAT1, CRABP2, and SPB5, were validated by western blotting (Fig. 3a). Because this validation method was not structure specific, candidates of subtype-specific protein modification (i.e. only one of multiple conformations was altered) were not selected for analysis. Figure 3(b) shows the box-plot of the expression levels of each protein for each of the four subtypes of EOC, quantitated by normalizing the bands against β-actin detected from the same membrane. The results show significant upregulation of ANXA4 and PSAT1 in clear cell carcinoma (P = 8.3E-07 and 4.9E-08,

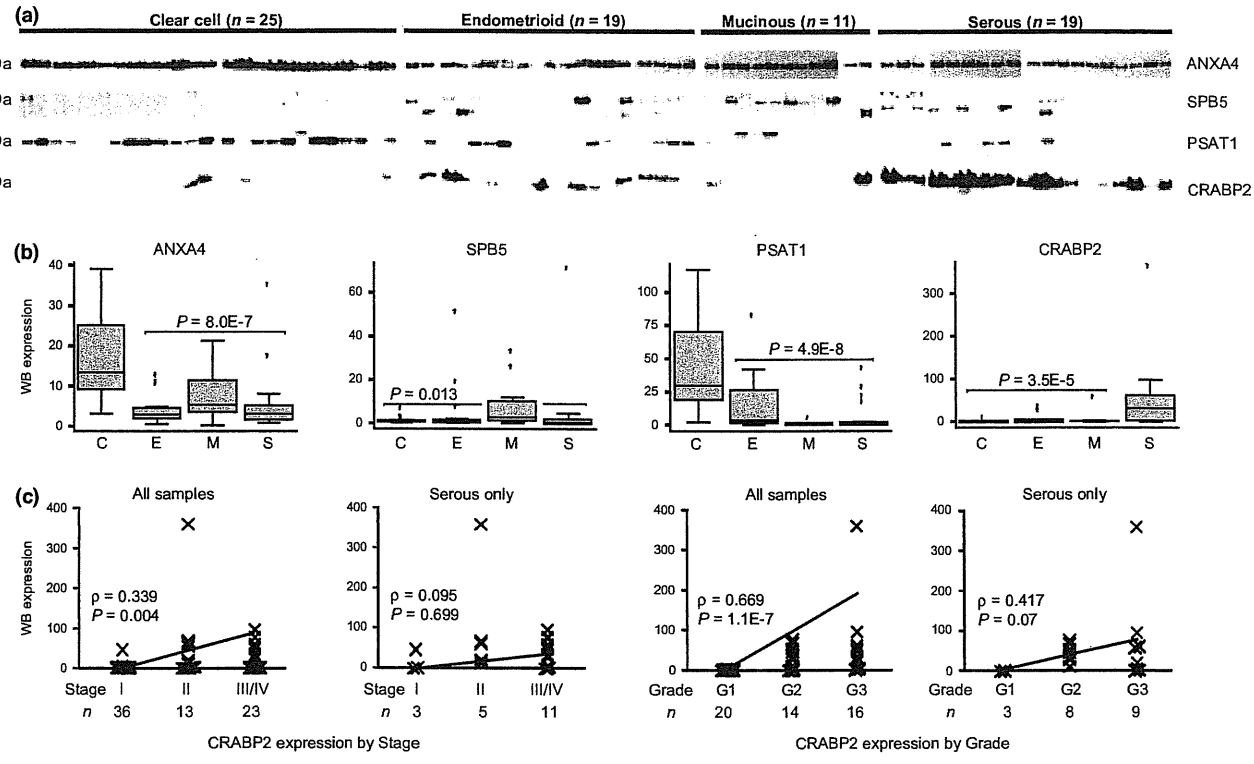

Fig. 3. Expression patterns for annexin A4 (ANXA4), cellular retinoic acid-binding protein 2 (CRABP2), serpin B5 (SPB5), and phosphoserine aminotransferase (PSAT1) were validated by western blotting using 74 tumor specimens. (a) Protein (5 μg) prepared from the same tissue lysate as that analyzed by two-dimensional (2D) gel electrophoresis was resolved by 10–16% tricine–SDS-PAGE, blotted onto a PVDF membrane, and detected by antibodies against each protein. Combined results of four independent blots are shown. One lane corresponds to one patient of the tumor type indicated at the top of the blots. (b) Box plots summarizing the expression of ANXA4, SPB5, PSAT1, and CRABP2 in each histological subtype. Expression was quantitated by normalizing the band volumes against the corresponding loading control band, detected by reprobing the same membrane. (c) Dot plots summarizing the expression of CRABP2 according to the International Federation of Gynecology and Obstetrics (FIGO) stage and tumor grade. The slope of the line of best fit is proportional to Spearman's correlation coefficient (ρ).

respectively, Mann–Whitney *U*-test), upregulation of CRABP2 in serous carcinoma (P = 3.5E-05), and upregulation of SPB5 in mucinous carcinoma (P = 0.013). Moreover, a possible correlation between the expression of these proteins and cancer stage (FIGO I, II, or III/IV) or grade (G1, G2 or G3; excluding clear cell carcinoma) was tested by Spearman's ρ calculation (Fig. 3c). There was significant correlation between CRABP2 expression and both cancer stage (ρ = 0.339, P = 0.004) and tumor grade (ρ = 0.669, P = 1.1E-7). However, this strongly reflected the characteristics of the serous subtype with which CRABP2 expression was associated. When the serous subtype was considered independently, there was no significant association between CRABP2 levels and tumor grade or stage. Instead, we observed a weak correlation between SPB5 expression and tumor grade in serous carcinoma (ρ = 0.499, P = 0.025).

Immunohistochemistry. We performed immunohistochemical staining for ANXA4. PSAT1, CRABP2, and SPB5 in formalin-fixed, paraffin-embedded tissue specimens representing clear cell, endometrioid, mucinous, and serous carcinoma to demonstrate differential staining and localization of candidate proteins (Fig. 4). Overall, staining was confined to the cancer cells of each subtype and the degree of staining was concordant with the results of western blotting. Clear cell carcinoma showed strongly positive staining for ANXA4 and PSAT1, and both cytosolic and nuclear staining were observed. Mucinous carcinoma was positive for ANXA4 and SPB5 (mainly in the cytosol), weakly positive for CRABP2, and negative for PSAT1. Serous carcinoma was very strongly positive for CRABP2, weakly positive for PSAT1, and negative for ANXA4 and SPB5. Endometrioid carcinoma was weakly positive for ANXA4, CRABP2, and PSAT1 and negative for SPB5. Using the panel of biomarkers, it was demonstrated that different tumor subtypes show characteristic immunohistochemical staining patterns. No stromal staining was observed throughout the analysis, except for serous stromal cells that showed a marginal response to CRABP2 staining.

Discussion

The present study is the first comprehensive proteomic characterization of ovarian cancer using clinical tumor specimens. The results identify molecular signatures that distinguish the histopathology of ovarian cancer. One advantage of 2-DE proteomic analysis over gene expression profiling using a cDNA microarray is that quantitative differences of target proteins are readily reproducible by antibody-based verification, and this was clearly illustrated in the present study by western blotting (Fig. 3) and differential staining by immunohistochemistry (Fig. 4). Thus, proteomic profiling defined key "effector" proteins that could contribute directly to the histopathological and clinical differences in the various subtypes of ovarian cancers. Moreover, considering the growing attention towards post-transcriptional protein regulation in systems biology,[24] our proteomic data should complement previous studies by gene expression profiling and uniquely identify previously overlooked features.

In the present study, we identified ANXA4 and PSAT1 as the most quantitative signature that best delineated the

doi: 10.1111/j.1349-7006.2012.02224.x

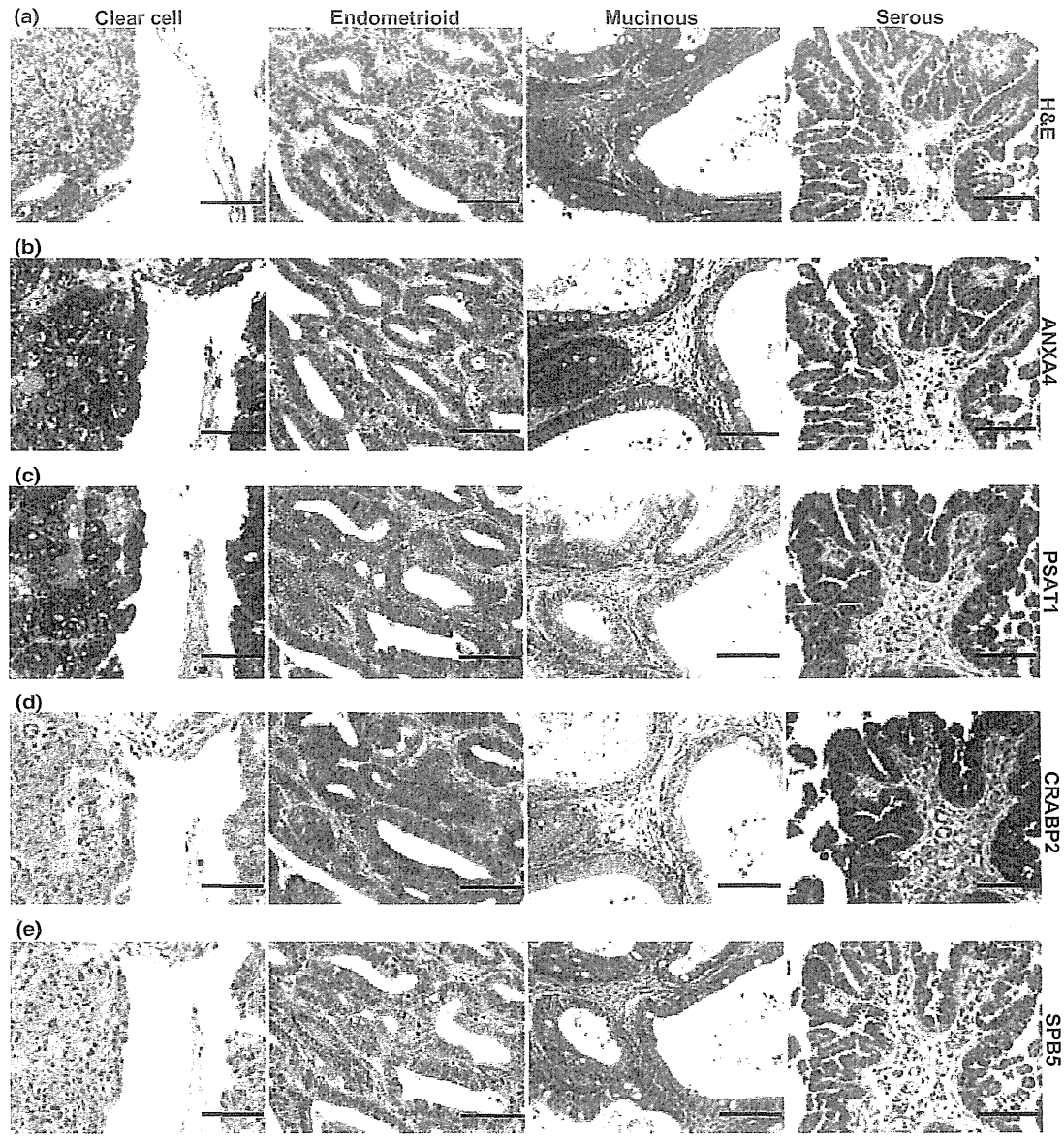

Fig. 4. Immunohistochemical analysis of primary epithelial ovarian carcinomas using formalin-fixed, paraffin-embedded tissue sections. (a) Representative H&E-stained images of clear cell, endometrioid, mucinous, and serous carcinomas. (b) Annexin A4 (ANXA4) staining was strongly positive in clear cell and mucinous carcinomas. (c) Phosphoserine aminotransferase (PSAT1) staining was strongly positive in clear cell carcinoma, weakly positive in endometrioid and serous carcinomas, and negative in mucinous carcinoma. (d) Cellular retinoic acid-binding protein 2 (CRABP2) staining was strongly positive in serous carcinoma, positive in endometrioid carcinoma, and marginally positive in mucinous carcinoma. (e) Serpin B5 (SPB5) staining was positive in mucinous carcinoma only. All sections were incubated for the same duration following 3′,3-diaminobenzidine development. Scale lines, 100 μm.

clear cell subtype from other subtypes. To our knowledge, upregulation of PSAT1 associated with ovarian cancer has not been reported previously. It is known that PSAT1 is part of the serine biosynthetic process[25] and its aberrant expression has been reported in colon cancer;[26] yet its role as an oncogene remains to be fully elucidated. A member of the calcium-dependent phospholipid-binding protein family, ANXA4 has been widely implicated to be associated with various cancers, including renal clear cell carcinoma,[27] pancreatic adenocarcinoma,[28] and ovarian clear cell carcinoma.[18] Although previous reports argue that ANXA4 expression directly confers cisplatin resistance,[29] which is a clinical characteristic of clear cell carcinoma, our western blotting data (Fig. 3) revealed very consistent basal expression of ANXA4 among all ovarian carcinoma samples tested. Moreover, on 2-DE separation, ANXA4 appeared in two distinct spots (Fig. 2a), arising from post-translational modification, and our immunohistological staining of ANXA4 suggested different localization according to EOC subtype. Such structural or functional changes to target molecules are promising biomarker candidates.

With regard to other proteins that were upregulated in clear cell carcinoma, 75% were metabolic enzymes involved in fundamental biological processes such as aerobic respiration (triosephosphate isomerase, L-lactate dehydrogenase B chain, carbonic anhydrase 2, transaldolase), cofactor processing (nicotinamide N-methyltransferase, catechol O-methyltransferase, methylcrotonoyl-CoA carboxylase beta chain, pyridoxal

kinase), and nucleoside metabolism (purine nucleoside phosphorylase, uridine monophosphate-cytidine monophosphate kinase 2). The wide spectrum of upregulated pathways suggests that the clear cell subtype of EOC is highly metabolically active, despite its slow tumor progression. Moreover, high levels of antioxidative enzymes, such as glutathione peroxidase 3, peroxiredoxin-2, peroxiredoxin-6, and superoxide dismutase, may be responsible for resistance to apoptosis induced by oxidative stress or chemotherapy.[30,31] These features are worth taking into consideration in the development of effective therapies against the clear cell subtype of EOC.

It is known that CRABP2 is strongly and specifically expressed in serous carcinoma; it contains a retinoic acid-binding domain and sensitizes the cellular response to the antiproliferative signaling by retinoic acid.[32] Whether serous carcinoma responds to retinoic acid signaling requires further investigation; if so, there is the chance that retinoic acid signaling would be a serous subtype-specific therapeutic target. In the present study, CRABP2 was almost entirely absent in clear cell carcinoma and exhibited the most significant difference between the serous and clear cell subtypes in our analysis. The absence of CRABP2 could explain a unique differentiation of clear cell carcinoma, and it could also be associated with endometriosis because CRABP2 is known to be strongly suppressed in endometriosis tissues.[33] Interestingly, the level of fatty acid binding protein 5, another retinoic acid signaling transducer that competes with CRABP2,[32] was slightly downregulated in clear cell carcinoma, but was generally uniform in other subtypes, suggesting that CRABP2 was deregulated independently of other retinoic acid signaling pathways. Similar deregulation has been reported in astrocytic gliomas, in which CRABP2 expression is associated with a poor prognosis.[34] Another intriguing protein upregulated in serous carcinoma is N^G,N^G-dimethylarginine dimethylaminohydrolase 2, which plays an important role in the nitric oxide signaling pathway via regulation of asymmetric dimethylarginine, an endogenous inhibitor of nitric oxide synthase.[35] Other proteins upregulated in the serous subtype of EOC include low molecular weight phosphotyrosine protein phosphatase, known to regulate EphA2-mediated signaling,[36] protein S100-A4, which is involved in nuclear factor-κB signaling, and cyclin-dependent kinase inhibitor 2A, which is involved in cell cycle regulation. Overall, the molecular signature of serous carcinoma is characterized by upregulation of proteins involved in multiple, apparently unrelated signaling pathways. Such prevalence of deregulated signaling pathways implicates dysfunction of the common central regulator, for example, TP53, which is mutated in most cases of serous carcinoma.[37]

Screening for mucinous-specific features was confounded by unmatched sample size. Nevertheless, SPB5 expressed aberrantly in mucinous carcinoma is known as a tumor suppressor gene in breast cancer and as an oncogene in various malignant cancers.[38] Our findings here agree with the recent study that reported aberrant SPB5 expression in mucinous ovarian carcinoma, where borderline tumors showed higher tendency of nuclear localization.[39] Moreover, our study revealed that endometrioid carcinoma exhibited a very heterogeneous molecular profile, with only seven proteins identified as endometrioid-specific features, and presented a wide range of principal components. We therefore speculate that there is the possibility that morphological classification of endometrioid carcinoma may be subdivided on the basis of specific molecular signatures to better characterize the clinical features.

In conclusion, the present proteomic characterization study provides evidence supporting the proposal that EOC subtypes are clinically distinct entities. Of particular interest are the correlations with the malignant and chemoresistant features of clear cell carcinoma. Better biomarkers associated with the different histopathological classifications of EOC, coupled with prognostic or chemosensitivity data, could suggest new avenues for clinical therapy. A molecular profile that correlates to histopathological classification would lead to a more detailed biological basis for this disease and eventually allow for the individualization of patient care.

Disclosure Statement

The authors have no conflict of interest to disclose.

References

1 Lawrenson K, Gayther SA. Ovarian cancer: a clinical challenge that needs some basic answers. *PLoS Med* 2009; **6**: e25.
2 Birrer MJ. The origin of ovarian cancer: is it getting clearer? *N Engl J Med* 2010; **363**: 1574–5.
3 Feeley KM, Wells M. Precursor lesions of ovarian epithelial malignancy. *Histopathology* 2001; **38**: 87–95.
4 Nagle CM, Olsen CM, Webb PM, Jordan SJ, Whiteman DC, Green AC. Endometrioid and clear cell ovarian cancers: a comparative analysis of risk factors. *Eur J Cancer* 2008; **44**: 2477–84.
5 Fehrmann RS, Li XY, van der Zee AG *et al.* Profiling studies in ovarian cancer: a review. *Oncologist* 2007; **12**: 960–6.
6 Takano M, Kikuchi Y, Yaegashi N *et al.* Clear cell carcinoma of the ovary: a retrospective multicentre experience of 254 patients with complete surgical staging. *Br J Cancer* 2006; **94**: 1369–74.
7 Pectasides D, Pectasides E, Psyrri A, Economopoulos T. Treatment issues in clear cell carcinoma of the ovary: a different entity? *Oncologist* 2006; **11**: 1089–94.
8 Ushijima K. Current status of gynecologic cancer in Japan. *J Gynecol Oncol* 2009; **20**: 67–71.
9 Fountain J, Trimble E, Birrer MJ. Summary and discussion of session recommendations. *Gynecol Oncol* 2006; **103**: S23–5.
10 Kobel M, Kalloger SE, Boyd N *et al.* Ovarian carcinoma subtypes are different diseases: implications for biomarker studies. *PLoS Med* 2008; **5**: e232.
11 Ono K, Tanaka T, Tsunoda T *et al.* Identification by cDNA microarray of genes involved in ovarian carcinogenesis. *Cancer Res* 2000; **60**: 5007–11.
12 Schwartz DR, Kardia SL, Shedden KA *et al.* Gene expression in ovarian cancer reflects both morphology and biological behavior, distinguishing clear cell from other poor-prognosis ovarian carcinomas. *Cancer Res* 2002; **62**: 4722–9.
13 Schaner ME, Ross DT, Ciaravino G *et al.* Gene expression patterns in ovarian carcinomas. *Mol Biol Cell* 2003; **14**: 4376–86.
14 Wamunyokoli FW, Bonome T, Lee JY *et al.* Expression profiling of mucinous tumors of the ovary identifies genes of clinicopathologic importance. *Clin Cancer Res* 2006; **12**: 690–700.
15 Welsh JB, Zarrinkar PP, Sapinoso LM *et al.* Analysis of gene expression profiles in normal and neoplastic ovarian tissue samples identifies candidate molecular markers of epithelial ovarian cancer. *Proc Natl Acad Sci USA* 2001; **98**: 1176–81.
16 An HJ, Kim DS, Park YK *et al.* Comparative proteomics of ovarian epithelial tumors. *J Proteome Res* 2006; **5**: 1082–90.
17 Morita A, Miyagi E, Yasumitsu H, Kawasaki H, Hirano H, Hirahara F. Proteomic search for potential diagnostic markers and therapeutic targets for ovarian clear cell adenocarcinoma. *Proteomics* 2006; **6**: 5880–90.
18 Zhu Y, Wu R, Sangha N *et al.* Classifications of ovarian cancer tissues by proteomic patterns. *Proteomics* 2006; **6**: 5846–56.
19 Gagne JP, Ethier C, Gagne P *et al.* Comparative proteome analysis of human epithelial ovarian cancer. *Proteome Sci* 2007; **5**: 16.
20 Benedet JL, Bender H, Jones H 3rd *et al.* FIGO staging classifications and clinical practice guidelines in the management of gynecologic cancers. FIGO Committee on Gynecologic Oncology. *Int J Gynaecol Obstet* 2000; **70**: 209–62.
21 Binns D, Dimmer E, Huntley R, Barrell D, O'Donovan C, Apweiler R. QuickGO: a web-based tool for Gene Ontology searching. *Bioinformatics* 2009; **25**: 3045–6.

doi: 10.1111/j.1349-7006.2012.02224.x

22 Shevchenko A, Tomas H, Havlis J, Olsen JV, Mann M. In-gel digestion for mass spectrometric characterization of proteins and proteomes. *Nat Protoc* 2006; **1**: 2856–60.
23 Pucci-Minafra I, Cancemi P, Albanese NN *et al.* New protein clustering of breast cancer tissue proteomics using actin content as a cellularity indicator. *J Proteome Res* 2008; **7**: 1412–8.
24 Schwanhausser B, Busse D, Li N *et al.* Global quantification of mammalian gene expression control. *Nature* 2011; **473**: 337–42.
25 Hart CE, Race V, Achouri Y *et al.* Phosphoserine aminotransferase deficiency: a novel disorder of the serine biosynthesis pathway. *Am J Hum Genet* 2007; **80**: 931–7.
26 Vie N, Copois V, Bascoul-Mollevi C *et al.* Overexpression of phosphoserine aminotransferase PSAT1 stimulates cell growth and increases chemoresistance of colon cancer cells. *Mol Cancer* 2008; **7**: 14.
27 Zimmermann U, Balabanov S, Giebel J *et al.* Increased expression and altered location of annexin IV in renal clear cell carcinoma: a possible role in tumour dissemination. *Cancer Lett* 2004; **209**: 111–8.
28 Shen J, Person MD, Zhu J, Abbruzzese JL, Li D. Protein expression profiles in pancreatic adenocarcinoma compared with normal pancreatic tissue and tissue affected by pancreatitis as detected by two-dimensional gel electrophoresis and mass spectrometry. *Cancer Res* 2004; **64**: 9018–26.
29 Kim A, Enomoto T, Serada S *et al.* Enhanced expression of Annexin A4 in clear cell carcinoma of the ovary and its association with chemoresistance to carboplatin. *Int J Cancer* 2009; **125**: 2316–22.
30 Saga Y, Ohwada M, Suzuki M *et al.* Glutathione peroxidase 3 is a candidate mechanism of anticancer drug resistance of ovarian clear cell adenocarcinoma. *Oncol Rep* 2008; **20**: 1299–303.
31 Chung YM, Yoo YD, Park JK, Kim YT, Kim HJ. Increased expression of peroxiredoxin II confers resistance to cisplatin. *Anticancer Res* 2001; **21**: 1129–33.
32 Schug TT, Berry DC, Shaw NS, Travis SN, Noy N. Opposing effects of retinoic acid on cell growth result from alternate activation of two different nuclear receptors. *Cell* 2007; **129**: 723–33.
33 Pavone ME, Reierstad S, Sun H, Milad M, Bulun SE, Cheng YH. Altered retinoid uptake and action contributes to cell survival in endometriosis. *J Clin Endocrinol Metab* 2010; **95**: E300–9.
34 Campos B, Centner FS, Bermejo JL *et al.* Aberrant expression of retinoic acid signaling molecules influences patient survival in astrocytic gliomas. *Am J Pathol* 2011; **178**: 1953–64.
35 Vallance P, Leiper J. Cardiovascular biology of the asymmetric dimethylarginine:dimethylarginine dimethylaminohydrolase pathway. *Arterioscler Thromb Vasc Biol* 2004; **24**: 1023–30.
36 Kikawa KD, Vidale DR, Van Etten RL, Kinch MS. Regulation of the EphA2 kinase by the low molecular weight tyrosine phosphatase induces transformation. *J Biol Chem* 2002; **277**: 39274–9.
37 Ahmed AA, Etemadmoghadam D, Temple J, *et al.* Driver mutations in TP53 are ubiquitous in high grade serous carcinoma of the ovary. *J Pathol* 2010; **221**: 49–56.
38 Khalkhali-Ellis Z. Maspin: the new frontier. *Clin Cancer Res* 2006; **12**: 7279–83.
39 Tsuji T, Togami S, Douchi T, Umekita Y. Difference in subcellular localization of maspin expression in ovarian mucinous borderline tumour. *Histopathology* 2009; **55**: 130–2.

Supporting Information

Additional Supporting Information may be found in the online version of this article:

Table S1. List of all ovarian carcinoma specimens used in the present study.

Table S2. Full list of the spot set used for biomarker screening shown with protein identity.

Please note: Wiley-Blackwell are not responsible for the content or functionality of any supporting materials supplied by the authors. Any queries (other than missing material) should be directed to the corresponding author for the article.

Tumor Biol. (2012) 33:1215–1222
DOI 10.1007/s13277-012-0369-4

RESEARCH ARTICLE

Cell surface expression of hyaluronan on human ovarian cancer cells inversely correlates with their adhesion to peritoneal mesothelial cells

Yutaka Tamada · Hideyuki Takeuchi · Nao Suzuki · Daisuke Aoki · Tatsuro Irimura

Received: 8 November 2011 / Accepted: 20 February 2012 / Published online: 6 March 2012

Abstract Eight of 15 human ovarian carcinoma cell lines were shown to express high levels of hyaluronan (HA) on their surfaces. The role of cell surface HA in its adhesion to mesothelial cells, which is potentially involved in peritoneal dissemination, was evaluated. Three human ovarian carcinoma cell lines, ES-2, MH, and KF cells, were repeatedly sorted into variant cell lines with high levels of cell surface HA (ES-2/HA+7, MH/HA+7, and KF/HA+7) and with low cell surface HA (ES-2/HA-7, MH/HA-7, and KF/HA-7). The ability of these cells to adhere to peritoneal mesothelial cells was compared. ES-2/HA+7, MH/HA+7, and KF/HA +7 cells were less adherent to mesothelial cells than the ES-2/HA-7, MH/HA-7, and KF/HA-7 cells. On ovarian carcinoma cells, high cell surface HA levels seem to inversely correlate with their capacity to adhere and disseminate to the peritoneum. Considering that peritoneum implantation is the primary ovarian cancer complication, HA cell surface expression may be considered a property associated with a less aggressive phenotype, which is contrary to the general perception that HA expression is associated with malignant progression.

Keywords Ovarian neoplasms · Peritoneal dissemination · Hyaluronan · CD44

Abbreviations
mAb monoclonal antibody
PBS phosphate-buffered saline

Introduction

Epithelial ovarian cancer spreads by tumor cell implantation on the mesothelial lining of the peritoneal cavity. In vitro studies have suggested that CD44, which is expressed on the surface of ovarian cancer cells, binds to the hyaluronan (HA) coat on mesothelial cells and may contribute to peritoneal metastasis [1–3]. Monoclonal antibodies against CD44 partially inhibit ovarian cancer cell adhesion to mesothelial cells and peritoneal implantation in mice [4, 5]. However, in many reports using the immunohistochemical staining method, high CD44 expression levels in ovarian cancer is not a negative prognostic indicator [6–10]. It is not likely that the interaction between the CD44 expressed on the ovarian cancer cell surface and the mesothelial cell HA results in a firm adhesion because the mesothelial cell HA coat is fluid in its physical property. Other molecular mechanisms such as integrins [11–13] and proteoglycans [14] may have to be considered to be involved in the implantation stage of ovarian cancer cells. In an immunohistochemical study, Anttila et al. demonstrated that high levels of stromal HA in ovarian cancer were associated with poor differentiation, serous histological type, advanced stage, and

Y. Tamada · H. Takeuchi · T. Irimura (✉)
Laboratory of Cancer Biology and Molecular Immunology,
Graduate School of Pharmaceutical Sciences,
The University of Tokyo,
7-3-1 Hongo, Bunkyo-ku,
Tokyo 113-0033, Japan
e-mail: irimura@mol.f.u-tokyo.ac.jp

Y. Tamada · D. Aoki
Department of Obstetrics and Gynecology, School of Medicine,
Keio University,
Tokyo 160-8582, Japan

N. Suzuki
Department of Obstetrics and Gynecology,
St. Marianna University School of Medicine,
Kawasaki 216-8511, Japan

large primary residual tumors, and that such associations were not correlated with the CD44 levels on cancer cells [15]. However, it remains unclear whether the stromal HA is produced by the ovarian cancer cells themselves.

In this study, by using 15 human ovarian carcinoma cell lines, we tested whether HA synthases (HAS) were expressed at the mRNA level, and we examined the potential role of cell surface HA in peritoneal implantation of ovarian carcinoma cells by testing their adhesion to peritoneal mesothelial cells. To our surprise, ovarian carcinoma cells containing high cell surface HA variants were less adherent to peritoneal mesothelial cells. Although this report is an in vitro study, is likely the first study to suggest that the tumor cell surface HA coat is not a pro-tumor molecule that is involved in peritoneal dissemination.

Materials and methods

Human ovarian cancer cell lines used

Origins and characteristics of 15 human ovarian carcinoma cell lines used in the present study were described previously [16]. RMG-I (No. 1), RMG-II (No. 2), RMUG-S (No. 6), RMUG-L (No. 7), and RTSG (No. 12) cells were established in Dr. Shiro Nozawa's laboratory in Keio University School of Medicine. MCAS (No. 8) cells were purchased from the Japanese Collection of Research Bioresources (Tokyo, Japan). ES-2 (No. 5) and OV1063 (No. 11) cells were purchased from the American Type Culture Collection (Rockville, MD). HUOCA-II (No. 4) and HKMOA (No. 9) cells were provided by Dr. Isamu Ishiwata (Ishiwata Hospital, Ibaraki, Japan). KK (No. 3), KF (No. 13), KFr (No. 14), and MH (No. 15) cells were provided by Dr. Yoshihiro Kikuchi (National Defense Medical College, Saitama, Japan). OMC-3 (No. 10) cells were provided by Dr. Masatsugu Ueda (Osaka Medical College, Osaka, Japan). All cells were cultured in a 1:1 (*v*/*v*) mixture of Dulbecco's modified Eagle's minimum essential medium and Ham's F-12 (DMEM/F12) supplemented with 10 % fetal bovine serum (Intergen, Purchase, NY) under 5 % carbon dioxide. The cells were mycoplasma-free as determined by the use of a Mycoplasma detection kit (Boehringer Mannheim, Mannheim, Germany).

Flow cytometric analysis

Flow cytometric analysis was performed by Epics Coulter XL (Beckman Coulter, Fullerton, CA) to determine the expression of the cell surface adhesion molecules. Anti-human CD44 antibody (clone OS/37), biotinylated HA binding protein (HABP), anti-human β1-integrin antibody (clone SG/19), and anti-heparan sulfate antibody (clone F58-10E4) were purchased from Seikagaku (Tokyo, Japan). The anti-E-selectin mAb [17] was provided by Dr. Tamatani (Takeda Chemical Industry, Tokyo, Japan).

An indirect immunofluorescence method was used to stain cells with either primary antibodies or biotinylated HABP (stained for 30 min on ice) followed by the addition of affinity purified fluorescein-conjugated goat anti-mouse immunoglobulin (Cappel, West Chester, PA) or FITC-Streptavidin (Zymed, South San Francisco, CA) secondary antibodies, respectively.

Reverse transcription-polymerase chain reaction analysis for CD44 and HAS1, 2, and 3 mRNA

Total RNA was isolated by using an Ultraspec RNA kit (Biotecx, Houston, TX). To avoid DNA contamination, the total RNA was treated with 100 U/ml DNase I, RNase-free (Boehringer) for 30 min at 37°C. One microgram of total RNA was reverse-transcribed with 5 U of M-MLV RTase in buffer containing 50 mM Tris-HCl (pH 8.3), 3 mM MgCl2, 75 mM KCl, 20 mM DTT (Gibco BRL, Gaithersburg, MD), 0.5 mM dNTPs (Amersham, Uppsala, Sweden), 0.05 U/μl RNase inhibitor (Takara Shuzo, Shiga, Japan), and 1 mg/ml pdT12-18 primer (Amersham, Uppsala, Sweden) in a final volume of 20 μl at 37°C for 90 min. Five percent of the obtained cDNA was PCR-amplified using 0.1 U/μl Taq polymerase (Perkin-Elmer, Emeryville, CA) in 10 mM Tris-HCl (pH 8.3), 50 mM KCl, 1.5 mM $MgCl_2$, 0.001 % gelatin, 0.2 mM dNTPs, and a 0.25–0.5 μM concentration of the respective 5′- and 3′-external primers. PCR amplification of CD44 cDNA transcripts was performed using two primers that flank the insertion site of alternatively spliced exons [10]. The primer sequences (5′ to 3′ orientation) were gacacatattgcttcaatgcttcagc and gatgccaagatgatcagccattctggaat. Thirty-five PCR cycles were performed under the following conditions: denaturation at 94°C for 1 min, annealing at 64°C for 1 min, and elongation at 72°C for 1 min. The PCR reaction products were analyzed by electrophoresis in 1.5 % agarose gel with a 100-bp ladder used as a marker (Gibco-BRL).

The oligonucleotide primer pairs specific for the respective human HAS genes were designed according to Spicer et al. as follows: Human HAS1, HAS1F 5′gtgcttctgtcgctctacgcg3′, and HAS1R 5′ccagtcccaatatagtccagactg3′ [nt positions 1410-1431 and 1940-1917] [18, 19], which amplified a 550-bp fragment; human HAS2, HAS2F 5′ggtgtgttcagtgcattagtgga3′, and HAS2R 5′tagccatctgagatactctataggt3′ [nt positions 1359-1382 and 1579-1555] [20], which amplified a 220-bp fragment; human HAS3, HAS3F 5′tgtgcagtgtattagtgggccct3′, and HAS3R 5′gttgagccaccggaggtacttag3′ [21], which amplified a 220-bp fragment. The cycling parameters for each primer pair were as follows: 35 cycles of 94°C for 1 min; 67°C (HAS1),

63°C (HAS2), or 65°C (HAS3) for 1 min; and 72°C for 1 min followed by a final extension step at 72°C for 7 min [22].

Selection of high or low expression variant sublines of cell surface hyaluronan from parental cell lines

ES-2 and MH cells were grown to 90 % confluence in 100-mm plates, released from the plate with 0.05 % Trypsin/0.02 % EDTA, and centrifuged into a pellet containing approximately 10×10^6 cells. The cells were resuspended in a solution of biotinylated HABP (1 ml of 10 μg/ml) and incubated at 4°C for 30 min. After washing, the cells were incubated at 4°C for 30 min with FITC-streptavidin (1 ml of 10 μg/ml, ZYMED). The stained cells were kept on ice and processed for cell sorting (Epics Elite, Beckman Coulter) within 1 h. Among the living cells, 5 % with highest or lowest fluorescence were chosen and sorted at a flow rate of 15,000–25,000 cells/s. Approximately 50,000 cells with high or low cell surface HA levels were collected and cultured in the media indicated above. The cells were subjected to repeated sorting when enough cell numbers were obtained at each cycle. After the seventh cycle, the resulting cells expressed either high or low cell surface HA levels, and the levels appeared to be stable. These cells were termed HA+7 and HA-7 variant cells for those containing high and low HA levels, respectively.

Preparation of peritoneal mesothelial cells

Human peritoneal mesothelial cells were obtained from patients with ovarian cancer localized in the ovary under informed consent. Mesothelial cell separation was performed according a previously described protocol [23, 24]. Briefly, the resected omentum was incubated in a 0.25 % trypsin/0.02 % EDTA solution for 20 min. A single cell suspension was obtained by filtration through an 80-μm mesh, dilution in DMEM/F12 medium containing 20 % FCS, and collection by centrifugation. The pellet containing mesothelial cells was resuspended in the medium and cultured until mesothelial cell monolayers were observed. Before the first passage, an antibiotic cocktail consisting of ampicillin sodium (50 mg/ml, Sigma Chemical, St. Louis, MO), streptomycin sulfate (100 mg/ml, Sigma), and amphotericin B (1 mg/ml, Sigma) was added to the medium (1:1,000 dilution). These cells were used at passages between 2 and 5.

In vitro peritoneal implantation model

The adhesion of ovarian cancer cells to monolayers of mesothelial cells was performed as described below. Ovarian cancer cells (5×10^6 cells/1 ml FCS-free medium) were mixed with 3 μl of a 1 mM BCECF-AM DMSO solution (Dojin, Kumamoto, Japan) and incubated for 30 min at 37° C. The labeled cells were centrifuged and washed with phosphate-buffered saline (PBS) and then resuspended in FCS-free medium for the experiment. Monolayers of peritoneal mesothelial cells were grown in 24-well plates. Labeled cancer cells (5×10^5 cells/1 ml FCS-free medium) were added and incubated at 37°C under rotation at 80 rpm using a rotary shaker (Multi Shaker MS-1, Shimadzu, Tokyo, Japan) to provide weak shear force. After incubating for 30 min, all wells were filled with DMEM/F12 medium and sealed using a Plate Seal MS-30010 (Sumitomo Bakelite, Tokyo, Japan). The plates were inverted and centrifuged at 250 rpm for 5 min. The cancer cells that did not adhere to the mesothelial cells were then spun down to the top of each well and the medium of each well were removed. The number of attached cells was counted using phase-contrast and fluorescence microscopy using a×20 magnification objective lens. The median number of attached cells in eight randomly selected visual fields was used as the indicator of adhesion.

Cell motility measured in vitro

We assessed motility of selected cells using Boyden chambers with 12 μm Millicell (Millipore Corporation, Bedford, MA). Lower chambers (1,500 μl) were filled with cell culture media (DMEM/F12 supplemented with 10 % fetal bovine serum). The upper chamber contained 5×10^4 cells/well and 500 μL of cell culture media. After incubation at 37°C for 24 h, the inserted chambers were removed and the number of cells in the lower chambers was counted. These assays were performed in triplicate.

Statistical analysis

Statistical analysis was performed using the unpaired Mann–Whitney *U* test or Fisher's exact probability test. *P* values less than 0.05 were considered to be significant.

Results

The cell surface molecules of peritoneal mesothelial cells, which were derived from human omentum, were characterized by flow cytometer. As shown in Fig. 1, CD44, β1-integrin, and heparan sulfate were expressed at high levels on the cell surface, whereas the HA level was low, and E-selectin was undetectable. These results were consistent with previous reports [1, 25].

Fifteen ovarian cancer cell lines were examined for their HA cell surface levels, as above. As shown in Fig. 2, ES-2, RMUG-L, HKMOA, KF, KFr, and MH cells had high HA levels, while the levels on OV1063 and RTSG cells were

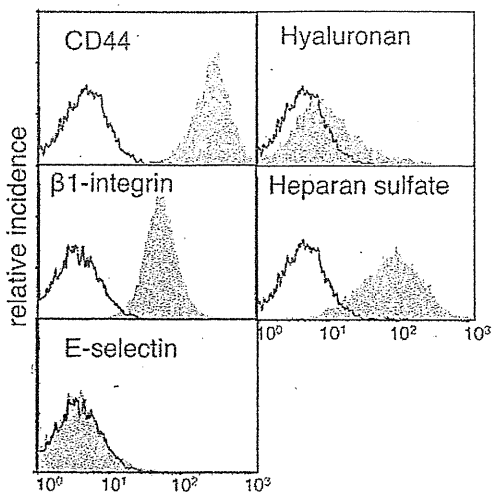

Fig. 1 Cell surface expression of CD44, HA, β1-integrin, heparan sulfate, and E-selectin on mesothelial cells derived from human omentum as determined by flow cytometric analysis. The *open areas* in each histogram represent the negative controls, and the *filled areas* represent antibody binding

intermediate. The HA expression levels on RMG-I, RMG-II, KK, HUOCA-II, RMUG-S, MCAS, and OMC-3 cells were low or undetectable.

The mRNA expression levels of *HAS1*, *HAS2*, *HAS3*, and *CD44*, which contains variant exons, were examined by reverse transcription-polymerase chain reaction (RT-PCR). Glyceraldehyde-3-phosphate dehydrogenase (*GAPDH*) was used as the loading control. As shown in Fig. 3, *HAS1* mRNA expression (550 bp) was not detected in any of the 15 cell lines. However, *HAS2* mRNA (220 bp) was detected at high levels in ES-2 and OV1063 cells and at relatively low levels in RMG-I, RMG-II, HUOCA-II, MCAS, RTSG, KFr, and MH cells. The levels of *HAS3* mRNA (220 bp) were high in all cell lines except for HUOCA-II cells. *CD44H* mRNA expression (the lowest band; 482 bp) was detected in all cell lines tested except HUOCA-II cells. As an internal control, *GAPDH* expression was confirmed in all cell lines (Fig. 3). As negative controls, samples treated without reverse transcriptase were assessed, and none of the *HAS* genes products were amplified (data not shown). The absence of *HAS1* mRNA was confirmed with primers that were used in another previous report [26] (data not shown). There was no clear correlation between *HAS2* or *HAS3* mRNA expression and the HA cell surface level.

To examine the potential role of cell surface HA in peritoneal dissemination, which is the most characteristic feature among ovarian cancer metastases, we selected variant cells that express high and low HA cell surface levels from the MH, ES-2, and KF cell lines. The cells stained with biotinylated HABP were repeatedly selected by a cell sorter. After seven selection cycles, cells stably expressing high or low HA cell surface levels were obtained and defined as MH/HA+7 and MH/HA-7 cells, ES-2/HA+7 and ES-2/HA-7 cells, and KF/HA+7 and KF/HA-7 cells, respectively (Fig. 4). Although we also attempted to separate high and low cell surface HA variants from RTSG and OV1063 cells, stable variant cells were not obtained (data not shown).

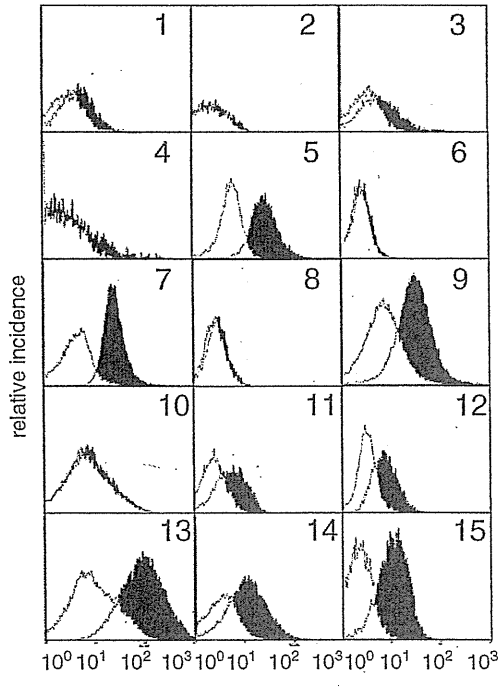

Fig. 2 Cell surface HA expression levels of 15 human ovarian cancer cell lines as determined by flow cytometry. *White areas* in the histograms show negative controls. *Black areas* show the HA levels revealed by HABP binding. *1* RMG-I cells; *2* RMG-II cells; *3* KK cells; *4* HUOCA-II cells; *5* ES-2 cells; *6* RMUG-S cells; *7* RMUG-L cells; *8* MCAS cells; *9* HKMOA cells; *10* OMC-3 cells; *11* OV1063 cells; *12* RTSG cells; *13* KF cells; *14* KFr cells; and *15* MH cells

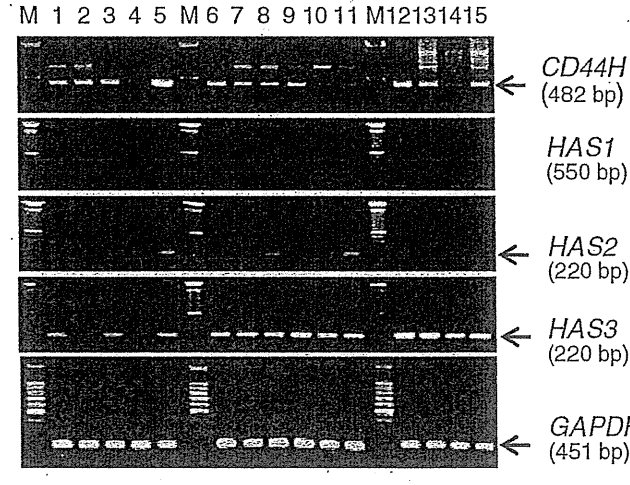

Fig. 3 Expression of *CD44H*, *HAS1*, *HAS2*, and *HAS3* mRNA by RT-PCR in 15 ovarian carcinoma cell lines. *M* molecular weight markers. *1* RMG-I cells; *2* RMG-II cells; *3* KK cells; *4* HUOCA-II cells; *5* ES-2 cells; *6* RMUG-S cells; *7* RMUG-L cells; *8* MCAS cells; *9* HKMOA cells; *10* OMC-3 cells; *11* OV1063 cells; *12* RTSG cells; *13* KF cells; *14* KFr cells; and *15* MH cells

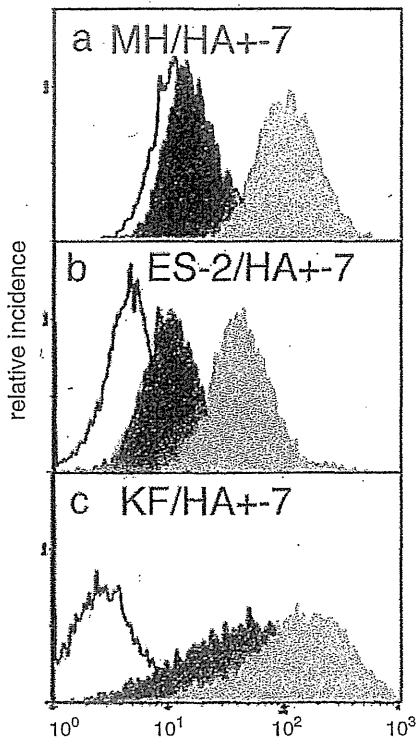

Fig. 4 Cell surface HA levels on high and low HA variant MH, ES-2, and KF cells. The amount of cell surface HA was detected by biotinylated HABP. *HA+7* represents variant cells obtained after seven cell sorting cycles for high cell surface HA and is shown with *gray areas* in the histograms. *HA-7* represents variant cells obtained after seven cell sorting cycles for low HA levels and is shown as *black areas* in the histograms. The *open areas* in the histograms show the control levels, which lack HABP addition

We investigated peritoneal implantation using an in vitro model. In the peritoneal cavity, the intestines move continuously by peristalsis. Therefore, floating cancer cells are always under shear stress. To mimic this condition, we performed adhesion assays under a weak shear force by using a rotating platform. As shown in Fig. 5, 69.7±6.6 (mean±SD) ES-2/HA+7 cells attached to mesothelial cell monolayers 30 min after 5×10^5 cells were seeded, whereas 254.5±18.3 (mean±SD) ES-2/HA-7 cells attached at the same time point. When MH/HA+7 cells and MH/HA-7 cells were compared, the numbers of attached cells were 6.2±0.9 (mean±SD) and 53.9±9.2 (mean±SD), respectively. When KF/HA+7 cells and KF/HA-7 cells were compared, 110.2±32.0 (mean±SD) and 491.0±37.2 (mean±SD) cells, respectively, attached. Therefore, for all three pairs of cell surface HA variants tested, the adhesive capacity of cancer cells to mesothelial cells was greater for the HA-7 variants as compared with the HA+7 variants.

We also investigated motility of these variants because the levels of cell surface HA potentially determine cell motility. MH/HA+7 and MH/HA-7 cells were tested for random motility with Boyden chambers. Figure 6 shows that significantly greater numbers of MH/HA+7 cells migrated to lower chambers. Such a difference may be due to increased motility or to the smaller size and round shape of MH/HA+7 cells compared to MH/HA-7 cells.

Discussion

HA is a polysaccharide [27] that is present in the extracellular matrix of epithelial and neural tissues, and it is abundantly localized in connective tissues. HA is known to control cell migration, differentiation, and proliferation [28], thereby influencing tissue morphogenesis, wound healing, and tumor growth [29, 30]. Tumor-associated extracellular matrices are often highly enriched for HA due to tumor-induced HA synthesis in normal fibroblasts and HA production by the tumor cells themselves [31]. A correlation between the HA level and tumor invasiveness has been

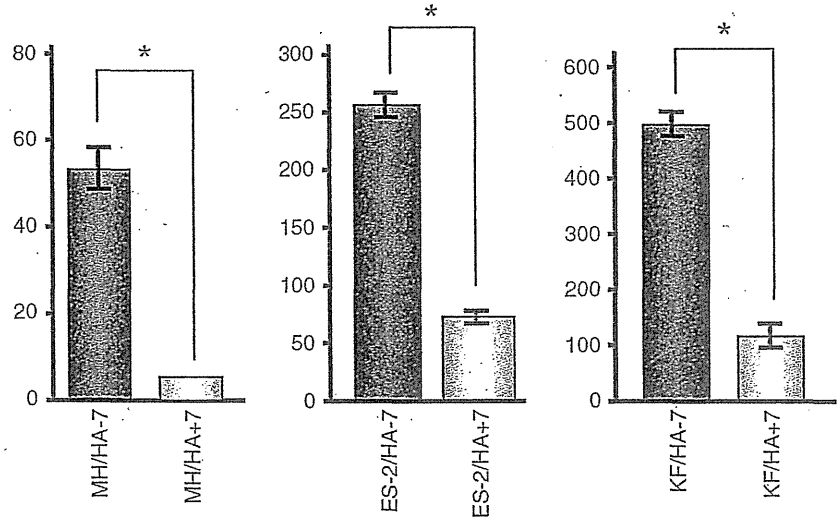

Fig. 5 Number of adherent ovarian carcinoma cells on the mesothelial cell monolayer 30 min after seeding 5×10^5 cells. The significance of the difference was determined by the Mann–Whitney *U* test. *Asterisks* indicate that the differences were statistically significant ($p<0.01$)

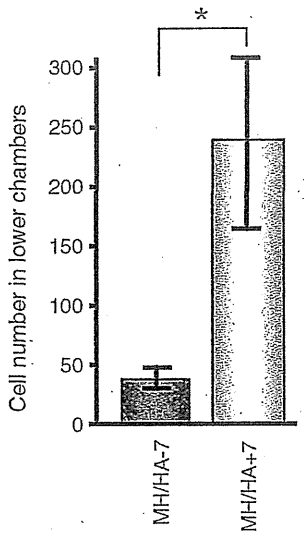

Fig. 6 Number of ovarian carcinoma variant MH/HA-7 and MH/HA +7 cells migrated through Nucleopore membranes 24 h after seeding 5×10^4 cells. The significance of the difference was determined by the Mann–Whitney *U* test. *Asterisks* indicate that the differences were statistically significant ($p<0.01$)

demonstrated in both human and mouse melanoma cells [30, 32]. The presence of HA on tumor cell surfaces is common and is thought to facilitate the interaction of these cells with host cells that express CD44 [30].

HA biosynthesis is controlled by three HASs in humans, HAS1, HAS2, and HAS3, and the properties of the unique products of these enzymes may elicit different functions [18–21]. The pericellular coats formed by *HAS1* transfectants were significantly thinner than those formed by *HAS2* or *HAS3* transfectants. Analysis of the size distribution of the in vitro generated HAs by these recombinant proteins has demonstrated that HAS3 synthesized HA with a molecular mass that is between 1×10^5 and 1×10^6 Da and shorter than those synthesized by HAS1 and HAS2, which have molecular masses between 2×10^5 and 2×10^6 Da [33]. HA overexpression by *HAS1* transfection has resulted in increased lung metastasis [34]. Increased HA production by *HAS2* transfection into human HT1080 cells promotes anchorage-independent growth and tumorigenicity [35]. Antisense *HAS3* inhibition has decreased pericellular HA retention and secretion, and it inhibited the anchorage-independent growth of colon carcinoma cells [36].

Although the biological properties of HA are likely to be dependent on its length, which is linked to the type of HAS that produces HA, the *HAS* gene expression profile in each cancer and each cancer cell is previously unknown. In this study, we used 15 human ovarian cancer cell lines and found that most of them primarily express *HAS3* and to a lesser extent, *HAS2*, but not *HAS1*. Thus, the lengths of HAs produced by ovarian cancer cells are likely to be short. We also found that HA was localized to the surface of ovarian carcinoma cell lines using flow cytometry. Absence of clear correlations between cell surface levels of HA and HAS transcripts suggested that each cell has unique degradation activity for HA. However, our preliminary experiments by the use of HA zymography [37] indicated that none of these cells produced a detectable level of hyaluronidase. Hyaluronidase purified from bovine testis was used as a positive control. Regulation of HA biosynthesis and its cell surface display by ovarian carcinoma cells may not be simple.

The peritoneal mesothelial cells we used showed a high level of expression of CD44, heparan sulfate, and β1-integrin on the cell surface, and no E-selectin. Surprisingly, our flow cytometric analysis of mesothelial cells indicated that the cell surface level of HA was low on these cells. These results are consistent with previous reports that have shown that the surface levels of β1-integrin, CD44, ICAM-1, and VCAM-1 were high on all mesothelial preparations, but those of E-selectin, P-selectin, sialyl Lewis^a, and sialyl Lewis^X were low [1, 25].

The degree of adhesion of ovarian carcinoma cells to mesothelial cells has been previously reported to be independent of the amount of cell surface CD44 [38]. Thus, we hypothesized that the HA on ovarian cancer cells influences their ability to adhere to CD44 on peritoneal mesothelial cells. In the present report, we established high and low HA expressing variant ovarian carcinoma cells by repeated cell sorting. Adhesion assays were performed under mild shear forces. The results of our study were unexpected; we found that ovarian cancer variant cells with high levels of cell surface HA were less adhesive to mesothelial cells than those with low HA. High HA expressing cells were more motile than low HA cells as determined by the Boyden chamber assays. Jones LM et al. have previously reported that HA secreted by mesothelial cells acts as a natural barrier to ovarian cancer cell adhesion [39]. Though their methods were different from ours, our findings support their results. A greater numbers of MH/HA+7 cells migrated through pored membranes in a common motility assay than MH/HA-7 cells. This does not necessarily mean that MH/HA+7 cells are more malignant because peritoneal implantation, which does not require high motility, is the primary cause of complication in ovarian carcinomas.

In conclusion, we show for the first time that ovarian carcinoma cell surface HA acts as a negative regulator of peritoneal implantation by reducing the capacity of tumor cells to adhere to mesothelial cells, thus acting as an antagonist of malignant behavior. However, tumor cell surface HA is known to block killing by cytotoxic lymphocytes, which provides support for tumor survival in the circulation [40]. Newly synthesized HA at the leading edge is known to support invasion of the extracellular matrix by tumor cells [41]. Therefore, tumor cell surface HA should be considered a double-edged sword that has pro and anti-tumor properties during ovarian cancer progression.

Acknowledgments We thank Ms. Kyoko Sakai and Ms. Miyuki Ikeda for their assistance in the preparation of this manuscript. This work was supported in part by grants-in-aid from the Ministry of Education, Science, Sports and Culture of Japan.

References

1. Cannistra SA, Kansas GS, Niloff J, DeFranzo B, Kim Y, Ottensmeier C. Binding of ovarian cancer cells to peritoneal mesothelium in vitro is partly mediated by CD44H. Cancer Res. 1993;53:3830–8.
2. Gardner MJ, Catterall JB, Jones LM, Turner GA. Human ovarian tumour cells can bind hyaluronic acid via membrane CD44: a possible step in peritoneal metastasis. Clin Exp Metastasis. 1996;14:325–34.
3. Catterall JB, Gardner MJ, Jones LM, Turner GA. Binding of ovarian cancer cells to immobilized hyaluronic acid. Glycoconj J. 1997;14:647–9.
4. Lessan K, Aguiar DJ, Oegema T, Siebenson L, Skubitz AP. CD44 and beta1 integrin mediate ovarian carcinoma cell adhesion to peritoneal mesothelial cells. Am J Pathol. 1999;154:1525–37.
5. Strobel T, Swanson L, Cannistra SA. In vivo inhibition of CD44 limits intra-abdominal spread of a human ovarian cancer xenograft in nude mice: a novel role for CD44 in the process of peritoneal implantation. Cancer Res. 1997;57:1228–32.
6. Sillanpaa S, Anttila MA, Voutilainen K, Tammi RH, Tammi MI, Saarikoski SV, Kosma VM. CD44 expression indicates favorable prognosis in epithelial ovarian cancer. Clin Cancer Res. 2003;9:5318–24.
7. Ross JS, Sheehan CE, Williams SS, Malfetano JH, Szyfelbein WM, Kallakury BV. Decreased CD44 standard form expression correlates with prognostic variables in ovarian carcinomas. Am J Clin Pathol. 2001;116:122–8.
8. Berner HS, Davidson B, Berner A, Risberg B, Kristensen GB, Trope CG, Van de Putte G, Nesland JM. Expression of CD44 in effusions of patients diagnosed with serous ovarian carcinoma—diagnostic and prognostic implications. Clin Exp Metastasis. 2000;18:197–202.
9. Saegusa M, Machida D, Hashimura M, Okayasu I. Cd44 expression in benign, premalignant, and malignant ovarian neoplasms: relation to tumour development and progression. J Pathol. 1999;189:326–37.
10. Cannistra SA, Abu-Jawdeh G, Niloff J, Strobel T, Swanson L, Andersen J, Ottensmeier C. CD44 variant expression is a common feature of epithelial ovarian cancer: lack of association with standard prognostic factors. J Clin Oncol. 1995;13:1912–21.
11. Strobel T, Cannistra SA. Beta1-integrins partly mediate binding of ovarian cancer cells to peritoneal mesothelium in vitro. Gynecol Oncol. 1999;73:362–7.
12. Casey RC, Skubitz AP. CD44 and beta1 integrins mediate ovarian carcinoma cell migration toward extracellular matrix proteins. Clin Exp Metastasis. 2000;18:67–75.
13. Casey RC, Burleson KM, Skubitz KM, Pambuccian SE, Oegema Jr TR, Ruff LE, Skubitz AP. Beta 1-integrins regulate the formation and adhesion of ovarian carcinoma multicellular spheroids. Am J Pathol. 2001;159:2071–80.
14. Kokenyesi R. Ovarian carcinoma cells synthesize both chondroitin sulfate and heparan sulfate cell surface proteoglycans that mediate cell adhesion to interstitial matrix. J Cell Biochem. 2001;83:259–70.
15. Anttila MA, Tammi RH, Tammi MI, Syrjanen KJ, Saarikoski SV, Kosma VM. High levels of stromal hyaluronan predict poor disease outcome in epithelial ovarian cancer. Cancer Res. 2000;60:150–5.
16. Tamada Y, Iida S, Aoki D, Nozawa S, Irimura T. Carbohydrate epitopes and mucins expressed by 17 human ovarian carcinoma cell lines. Oncol Res. 1999;11:233–41.
17. Tamaru M, Tomura K, Sakamoto S, Tezuka K, Tamatani T, Narumi S. Interleukin-1beta induces tissue- and cell type-specific expression of adhesion molecules in vivo. Arterioscler Thromb Vasc Biol. 1998;18:1292–303.
18. Shyjan AM, Heldin P, Butcher EC, Yoshino T, Briskin MJ. Functional cloning of the cDNA for a human hyaluronan synthase. J Biol Chem. 1996;271:23395–9.
19. Itano N, Kimata K. Molecular cloning of human hyaluronan synthase. Biochem Biophys Res Commun. 1996;222:816–20.
20. Watanabe K, Yamaguchi Y. Molecular identification of a putative human hyaluronan synthase. J Biol Chem. 1996;271:22945–8.
21. Spicer AP, Olson JS, McDonald JA. Molecular cloning and characterization of a cDNA encoding the third putative mammalian hyaluronan synthase. J Biol Chem. 1997;272:8957–61.
22. Spicer AP, Seldin MF, Olsen AS, Brown N, Wells DE, Doggett NA, Itano N, Kimata K, Inazawa J, McDonald JA. Chromosomal localization of the human and mouse hyaluronan synthase genes. Genomics. 1997;41:493–7.
23. Takahashi K, Goto T, Mukai K, Sawasaki Y, Hata J. Cobblestone monolayer cells from human omental adipose tissue are possibly mesothelial, not endothelial. In Vitro Cell Dev Biol. 1989;25:109–11.
24. Pronk A, Leguit P, Hoynck van Papendrecht AA, Hagelen E, van Vroonhoven TJ, Verbrugh HA. A cobblestone cell isolated from the human omentum: the mesothelial cell; isolation, identification, and growth characteristics. In Vitro Cell Dev Biol. 1993;29A:127–34.
25. Gardner MJ, Jones LM, Catterall JB, Turner GA. Expression of cell adhesion molecules on ovarian tumour cell lines and mesothelial cells, in relation to ovarian cancer metastasis. Cancer Lett. 1995;91:229–34.
26. Simpson MA, Reiland J, Burger SR, Furcht LT, Spicer AP, Oegema Jr TR, McCarthy JB. Hyaluronan synthase elevation in metastatic prostate carcinoma cells correlates with hyaluronan surface retention, a prerequisite for rapid adhesion to bone marrow endothelial cells. J Biol Chem. 2001;276:17949–57.
27. Meyer K, Palmer JW. The polysaccharide of the vitreous humor. J Biol Chem. 1934;107:629–34.
28. Toole B. Glycosaminoglycans in morphogenesis. In: Hay E (ed), Cell biology of the extracellular matrix. Plenum Press 1982:259-294.
29. Mast BA, Diegelmann RF, Krummel TM, Cohen IK. Scarless wound healing in the mammalian fetus. Surg Gynecol Obstet. 1992;174:441–51.
30. Zhang L, Underhill CB, Chen L. Hyaluronan on the surface of tumor cells is correlated with metastatic behavior. Cancer Res. 1995;55:428–33.
31. Knudson CB, Knudson W. Hyaluronan-binding proteins in development, tissue homeostasis, and disease. FASEB J. 1993;7:1233–41.
32. van Muijen GN, Danen EH, Veerkamp JH, Ruiter DJ, Lesley J, van den Heuvel LP. Glycoconjugate profile and CD44 expression in human melanoma cell lines with different metastatic capacity. Int J Cancer. 1995;61:241–8.
33. Itano N, Sawai T, Yoshida M, Lenas P, Yamada Y, Imagawa M, Shinomura T, Hamaguchi M, Yoshida Y, Ohnuki Y, Miyauchi S, Spicer AP, McDonald JA, Kimata K. Three isoforms of mammalian hyaluronan synthases have distinct enzymatic properties. J Biol Chem. 1999;274:25085–92.
34. Itano N, Sawai T, Miyaishi O, Kimata K. Relationship between hyaluronan production and metastatic potential of mouse mammary carcinoma cells. Cancer Res. 1999;59:2499–504.
35. Kosaki R, Watanabe K, Yamaguchi Y. Overproduction of hyaluronan by expression of the hyaluronan synthase HAS2 enhances

anchorage-independent growth and tumorigenicity. Cancer Res. 1999;59:1141–5.
36. Bullard KM, Kim HR, Wheeler MA, Wilson CM, Neudauer CL, Simpson MA, McCarthy JB. Hyaluronan synthase-3 is upregulated in metastatic colon carcinoma cells and manipulation of expression alters matrix retention and cellular growth. Int J Cancer. 2003;107:739–46.
37. Podyma KA, Yamagata S, Sakata K, Yamagata T. Difference of hyaluronidase produced by human tumor cell lines with hyaluronidase present in human serum as revealed by zymography. Biochem Biophys Res Commun. 1997;241:446–52.
38. Catterall JB, Jones LM, Turner GA. Membrane protein glycosylation and CD44 content in the adhesion of human ovarian cancer cells to hyaluronan. Clin Exp Metastasis. 1999;17:583–91.
39. Jones LM, Gardner MJ, Catterall JB, Turner GA. Hyaluronic acid secreted by mesothelial cells: a natural barrier to ovarian cancer cell adhesion. Clin Exp Metastasis. 1995;13:373–80.
40. Toole BP, Biswas C, Gross J. Hyaluronate and invasiveness of the rabbit v2 carcinoma. Proc Natl Acad Sci USA. 1979;76:6299–303.
41. Rooney P, Kumar S, Ponting J, Wang M. The role of hyaluronan in tumour neovascularization (review). Int J Cancer. 1995;60:632–6.

Gynecologic Oncology 127 (2012) 338–344

Contents lists available at SciVerse ScienceDirect

Gynecologic Oncology

journal homepage: www.elsevier.com/locate/ygyno

Clinicopathological prognostic factors and the role of cytoreduction in surgical stage IVb endometrial cancer: A retrospective multi-institutional analysis of 248 patients in Japan

Takako Eto [a,*], Toshiaki Saito [a], Takahiro Kasamatsu [b], Toru Nakanishi [c], Harushige Yokota [d], Toyomi Satoh [e], Takayoshi Nogawa [f], Hiroyuki Yoshikawa [e], Toshiharu Kamura [g], Ikuo Konishi [h]

[a] Gynecology Service, National Kyushu Cancer Center, 3-1-1 Notame, Minami-ku, Fukuoka 811-1395, Japan
[b] Department of Gynecology, National Cancer Center Hospital, 5-1-1 Tsukiji, Chuo-ku, Tokyo 104-0045, Japan
[c] Department of Gynecology, Aichi Cancer Center Hospital, 1-1 Kanokoden, Chikusa Nagoya, Aichi, 464-8681, Japan
[d] Department of Gynecology, Saitama Cancer Center Hospital, 818 Komuro Ina, Kita-Adachi, Saitama, 362-0806, Japan
[e] Department of Obstetrics and Gynecology, University of Tsukuba, 1-1-1 Tennoudai, Tsukuba, Ibaraki 305-8575, Japan
[f] Gynecology Service, National Hospital Organization Shikoku Cancer Center, 160 Koh, Minami Umemoto-machi, Matsuyama, Ehime 791-0280, Japan
[g] Department of Obstetrics and Gynecology, Kurume University School of Medicine, 67 Asahi machi, Kurume, 830-0011, Japan
[h] Department of Gynecology and Obstetrics, Kyoto University Graduate School of Medicine, 54 Shogoin Kawahara-cho, Sakyo-ku, Kyoto 606-8507, Japan

HIGHLIGHTS

- A total of 248 patients with surgical stage IVb endometrial cancer were reviewed.
- Low grade endometrioid type was a good prognostic factor in this group.
- Cytoreduction and chemotherapy may improve survival even in metastatic disease.

ARTICLE INFO

Article history:
Received 16 June 2012
Accepted 12 August 2012
Available online 19 August 2012

Keywords:
Stage IVb endometrial cancer
Prognostic factor
Surgical cytoreduction
Extra-abdominal metastases

ABSTRACT

Objective. To evaluate clinicopathological prognostic factors and the impact of cytoreduction in patients with surgical stage IVb endometrial cancer (EMCA).

Methods. The records of 248 patients with stage IVb EMCA who underwent primary surgery including hysterectomy at multiple institutions from 1996 to 2005 were retrospectively analyzed. Data regarding disease distribution, surgical procedures, adjuvant therapy, and survival times were collected. Univariate and multivariate analyses were performed to identify factors associated with overall survival (OS).

Results. The median OS was 24 months. The most common histological types were endometrioid (grade 1: 15%, grade 2: 20%, grade 3: 24%) and serous (17%). The most common sites of intra-abdominal metastases were pelvis (65%), ovaries (58%), omentum (58%), retroperitoneal lymph nodes (52%), and upper abdominal peritoneum (44%). In 93 patients with extra-abdominal metastases, the most common site was the lung (n = 49). Complete resection of extra-abdominal metastases was achieved in only 13 patients. Complete resection of intra-abdominal metastases was achieved in 101 patients, 52 had ≤1 cm residual disease, and 95 had >1 cm residual disease; the median OS times in these groups were 48, 23, and 14 months, respectively ($p<0.0001$). Multivariate analysis showed that performance status, histology/grade, adjuvant treatment, and intra-abdominal residual disease were independent prognostic factors. Intra-abdominal residual disease was an independent prognostic factor in patients with and without extra-abdominal metastases.

Conclusions. Cytoreductive surgery and adjuvant therapy may improve survival in stage IVb EMCA, particularly in patients with favorable prognostic factors, even in the presence of extra-abdominal metastases.

Introduction

Endometrial cancer (EMCA) is commonly diagnosed at an early stage and has a favorable prognosis [1,2]. The treatment of early-stage EMCA is well established, but the most effective treatment strategies for stage IVb EMCA remain unclear. Stage IVb disease is rare, and the prognosis remains very poor. According to the International Federation of Gynecology and Obstetrics (FIGO) Annual Report, approximately 3% of EMCA patients are classified as stage IV [3]. The 5-year survival rate of surgical stage IVb patients is reportedly 20.1%, and the 4-year survival rate of clinical stage IVb patients is 7.7%. There are no data to

* Corresponding author. Fax: +81 92 551 4585.
E-mail address: teto@nk-cc.go.jp (T. Eto).

0090-8258/$ – see front matter © 2012 Elsevier Inc. All rights reserved.
http://dx.doi.org/10.1016/j.ygyno.2012.08.012

aid therapeutic decision-making in these patients, and there is no consensus regarding the most effective treatment strategies.

The population of patients with stage IVb EMCA is heterogeneous, as this stage includes patients with upper intra-abdominal dissemination and extra-abdominal metastases. Patients with stage IVb EMCA can therefore be divided into subgroups according to intra- and extra-abdominal disease. However, few published reports have described the specific disease distribution of surgical stage IVb EMCA patients [4–7].

Although the treatment of advanced EMCA is developing in a similar direction to the treatment of ovarian cancer, the role of surgery in the treatment of stage IVb EMCA is unresolved. Recently, several investigators have retrospectively evaluated the role of surgical cytoreduction in patients with stage IVb disease [4,7–12]. A meta-analysis [13] demonstrated that complete cytoreduction is associated with superior overall survival. However, previous studies have been based on populations selected for surgery, with relatively few extra-abdominal metastases. The lung is reportedly the main site of extrapelvic tumor spread, followed by multiple other sites [14]. The effectiveness of intra-abdominal cytoreductive surgery in patients with extra-abdominal metastases considered to be unresectable is unknown.

We hypothesized that clinicopathological characteristics and disease distribution are important when establishing treatment strategies for this disease. We conducted a multicenter study of stage IVb EMCA patients treated in Japan Clinical Oncology Group-related institutions. The primary objective of this study was to clarify the clinicopathological characteristics and disease distribution of surgical stage IVb EMCA patients. The secondary objective was to identify prognostic factors which affect survival and evaluate the impact of cytoreductive surgery on prognosis, including surgery in patients with extra-abdominal metastases.

Methods

Patients

We performed a retrospective review of all patients diagnosed with clinical or surgical FIGO 1988 stage IVb EMCA from 1996 to 2005 who were treated in 30 Gynecologic Cancer Study Group of Japan Clinical Oncology Group-related institutions. Patients with sarcoma were excluded. Patients with stage IVb EMCA who underwent primary surgery including hysterectomy and bilateral salpingo-oophorectomy were eligible.

A case report form was developed using data software (FileMaker-pro Version 6/8) to obtain equivalent data from multiple institutions. The investigation protocol, including the case report form, was approved by the Institutional Review Board of each institution.

Complete clinical data were collected by reviewing inpatient charts, operative records, original pathology reports, and outpatient records from each institution. The demographic data collected included: age, Eastern Cooperative Oncology Group (ECOG) performance status (PS), reproductive history, medical comorbidities, and body mass index (BMI). Pathological information was collected from the pathology reports of the preoperative endometrial biopsy and hysterectomy specimens. The sites and sizes of metastases, surgical procedures, and sites and maximum diameter of residual disease after surgery were collected from radiology reports, intraoperative findings, and pathology reports. Treatment data collected included details of postoperative adjuvant treatment. Follow-up was continued regularly at each institution. Follow-up information included the date and disease status at the last follow-up, or the date and cause of death.

Stage IVb metastases were divided into intra- and extra-abdominal disease. Metastasis to the liver surface was classified as intra-abdominal disease, and metastasis to the liver parenchyma was classified as extra-abdominal disease, following the classification for ovarian cancer. Postoperative residual disease was also divided into intra- and extra-abdominal disease. Remaining retroperitoneal lymphadenopathy and intrapelvic disease were classified as intra-abdominal residual disease. Patient outcomes were analyzed by overall survival (OS) time. OS was calculated from the date of surgery to the date of death or last contact.

Statistical analysis

The Kaplan–Meier method was used to estimate OS curves, and survival was compared among groups using the log-rank test. A p value of <0.05 was considered statistically significant. Multivariate Cox proportional hazards regression analyses were used to identify independent prognostic variables. Factors with a p value of <0.1 in univariate analyses were included in the multivariate analyses. All analyses were performed using SPSS statistical software (11.0.1 J; SPSS Inc., Chicago, IL).

Results

Patients and characteristics

We identified a total of 426 patients with stage IVb EMCA, of which 279 underwent primary surgery with curative intent as the initial treatment. After excluding 31 patients who did not undergo hysterectomy and cytoreductive surgery, 248 patients met the study inclusion criteria.

Detailed clinicopathological characteristics of the patients are listed in Table 1. The median age was 59 years (range: 30–89 years), and 91% had a pretreatment ECOG PS of 0/1. Mean BMI was 23.2 kg/m^2 (range: 15.1–35.8 kg/m^2). Medical comorbidities included hypertension in 19% of patients and diabetes in 9%. The most common histological subtype was endometrioid. There was a high frequency of poor histological factors, with endometrioid grade 3 (EMG3) or non-endometrioid

Table 1
Clinicopathological characteristics (n = 248).

Characteristic	n	(%)
Median age, years (range)	59(30–89)	
ECOG performance status		
0–1	226	(91)
2	17	(7)
3–4	4	(2)
Unknown	1	(<1)
Diabetes mellitus	22	(9)
Hypertension	47	(19)
Histological type		
Endometrioid	149	(61)
Serous	43	(17)
Clear cell	15	(6)
Carcinosarcoma	23	(9)
Other	18	(7)
Grade		
Endometrioid G1	36	(15)
Endometrioid G2	50	(20)
Endometrioid G3	60	(24)
Non-endometrioid	99	(40)
Unknown	3	(1)
Deep myometrial invasion	170	(69)
LVSI	173	(70)
Adjuvant therapy		
CT alone	185	(75)
RT alone	11	(4)
CT + RT	24	(10)
None	28	(11)
Chemotherapy regimen		
Taxane + platinum	115	(46)
AP ± α	79	(32)
Other	15	(6)

ECOG, Eastern Cooperative Oncology Group.
LVSI, lymphovascular space involvement.
CT, chemotherapy; RT, radiotherapy.
A P ± α, doxorubicin + platinum ± other.

histology, deep myometrial invasion, and positive lymphovascular space invasion (LVSI), each found in more than 60% of patients. Only 36 patients (15%) were classified as EMG1. The preoperative histological diagnosis was identical to the postoperative diagnosis in 150 patients (60%). Only 8 of 23 patients (35%) with carcinosarcoma were correctly diagnosed by preoperative endometrial biopsy.

Disease distribution

Disease distribution by anatomical region is shown in Table 2. Extra-abdominal metastases were documented in 93 patients (38%), of whom 71 (75%) had metastasis in only one anatomical region. The most common sites of extra-abdominal metastases were the lungs, supraclavicular lymph nodes, liver, and mediastinal lymph nodes. The majority of lung metastases were bilateral (36/49, 74%) and multiple (40/49, 82%). The diameter of lung metastasis was ≤1 cm in 19 patients, 1–2 cm in 20 patients, >2 cm in 9 patients, and unknown in 1 patient.

Intra-abdominal metastases beyond the pelvis were documented in 191 patients. The diameter of upper intra-abdominal metastases was >2 cm in 105 patients (55%), ≤2 cm in 72 patients (38%), and microscopic in 14 patients (7%). Intra-abdominal stage IVb disease was diagnosed on preoperative imaging in only 47 patients. Other intra-abdominal metastases not categorized as stage IVb disease were also frequently recognized (pelvic peritoneum, positive peritoneal washing cytology, ovaries, and retroperitoneal lymph nodes).

Table 2
Disease distribution.

Site of metastases	n	(%)
Stage IVb disease site		
Intra-abdominal alone	155	(62)
Extra-abdominal alone	57	(23)
Both	36	(15)
Extra-abdominal metastasis	93	(38)
1 region	71	(29)
2 regions	17	(7)
≥3 regions	5	(2)
Lung	49	(20)
Liver	12	(5)
Bone	7	(3)
Brain	3	(1)
Skin, umbilicus, breast	4	(2)
Conjunctiva	1	(<1)
Malignant pleural effusion	5	(2)
Supraclavicular lymph node	15	(6)
Mediastinal/axillary node	12	(5)
Inguinal node	10	(4)
Intra-abdominal metastasis	191	(77)
Sites staged as IVb		
Omentum	143	(58)
Macroscopic	125	(50)
Microscopic	18	(7)
Diaphragm	54	(22)
Peritoneum (upper abdomen)	109	(44)
Colon	7	(3)
Small intestine	3	(1)
Mesentery	6	(2)
Appendix	7	(3)
Sites staged as non-IVb		
Peritoneum (pelvis)	160	(65)
Retroperitoneal node	129	(52)
Para-aortic node	91	(37)
Pelvic node	115	(46)
Peritoneal washing cytology	156	(63)
Bowel mucosa	9	(4)
Bladder mucosa	2	(<1)
Ovary	144	(58)
Parametrium	28	(11)
Vagina	11	(4)

Surgical procedures and results

All 248 patients underwent surgical staging (Table 3). In addition to hysterectomy and bilateral salpingo-oophorectomy, cytoreductive procedures with the intent of maximum cytoreduction were performed in most patients. Resection of the colon, ileum, spleen, or diaphragmatic peritoneum was performed in 19 patients. After surgery, 101 patients (41%) had complete gross intra-abdominal resection and 52 (21%) had ≤1 cm residual disease.

To remove extra-abdominal metastases, some patients underwent resection of inguinal/supraclavicular lymph nodes, the umbilicus, or the abdominal wall. No patients underwent resection of lung or liver metastases. Complete resection of extra-abdominal metastases was achieved in only 13 patients.

Postoperatively, one patient with >2 cm residual disease died of disease progression on postoperative day 26. No major life-threatening complications occurred within 30 days after surgery.

Postoperative adjuvant therapy

Postoperative adjuvant therapy was administered to 220 patients (89%). The majority of these (n=185) were treated with chemotherapy alone. A variety of chemotherapy regimens were used including paclitaxel, docetaxel, carboplatin, cisplatin, doxorubicin, cyclophosphamide, ifosfamide, etoposide, CPT11, and 5-fluorouracil. The most commonly administered regimen was taxanes + platinum ± doxorubicin (n=115), followed by doxorubicin + platinum (AP) ± cyclophosphamide ± ifosfamide (n=79). Radiotherapy was administered to 35 patients, including external beam radiotherapy to the whole pelvis (n=23), para-aortic lesions (n=16), neck (n=6), bone (n=3), brain (n=2), and vaginal brachytherapy (n=2).

Clinical and pathological risk factors for survival

The median follow-up time among the censored patients was 41 months, and the median OS was 24 months (95% confidence interval [CI], 20–29 months). The causes of death were EMCA in 157 patients, other diseases in 2, and unknown in 3. At the last follow-up, 48 patients were alive with no evidence of disease, 33 were alive with disease, and 5 were alive with unknown disease status. There were no treatment-related deaths.

Table 3
Surgical procedures performed.

Procedure	n	(%)
Intra-abdominal		
Hysterectomy + BSO	248	(100)
Type of hysterectomy		
Simple	184	(74)
Subtotal	9	(4)
Modified-radical	49	(20)
Radical	6	(2)
Omentectomy/biopsy	157	(63)
Pelvic lymphadenectomy	157	(63)
Para-aortic lymphadenectomy	82	(33)
Resection of peritoneum	90	(36)
Appendectomy	30	(12)
Resection of colon/ileum	17	(7)
Colostomy/ileostomy	3	(1)
Splenectomy	1	(<1)
Diaphragm peritonectomy	1	(<1)
Resection of internal iliac artery	1	(<1)
Extra-abdominal		
Mastectomy	1	(<1)
Resection of umbilicus/skin	3	(1)
Resection of supraclavicular nodes	3	(1)
Resection of inguinal nodes	7	(3)

BSO, bilateral salpingo-oophorectomy.

Table 4
Univariate analyses for overall survival.

Variable	n	(%)[a]	Median OS (months) (95% CI)	Log-rank p[b]
Age				
≤59 years	134	(54)	29 (22–36)	
≥60 years	114	(46)	20 (13–28)	0.0675
ECOG performance status				
0–1	226	(91)	25 (20–31)	
2–4	21	(8)	11 (5–16)	0.0150
Stage IVb disease site				
Intra-abdominal alone	155	(62)	24 (19–29)	
Extra-abdominal alone	57	(23)	30 (0–61)	
Both	36	(15)	20 (9–31)	0.1283
Histological type				
Endometrioid	149	(60)	31 (21–40)	
Non-endometrioid	99	(40)	14 (7–22)	<0.0001
Histology and grade				
EMG1	36	(15)	79 (not estimated)	
EMG2	50	(20)	48 (28–68)	
EMG3 + non-EM	159	(64)	14 (8–21)	<0.0001
Myometrial invasion				
≤1/2	59	(24)	40 (28–53)	
>1/2	170	(69)	22 (16–7)	0.0108
LVSI				
Present	173	(70)	24 (19–8)	
Absent	27	(11)	58 (not estimated)	0.0037
Stage IVb disease site				
Extra-abdominal metastasis				
Positive	93	(38)	24 (15–4)	
Negative	155	(62)	24 (19–9)	0.3722
Intra-abdominal metastasis				
Positive	191	(77)	23 (19–27)	
Negative	57	(23)	30 (0–61)	0.0609
Site of metastasis				
Para-aortic lymph node				
Positive	91	(37)	21 (14–27)	
Negative	119	(48)	31 (17–45)	0.0086
Pelvic lymph node				
Positive	115	(46)	21 (14–28)	
Negative	104	(42)	32 (18–47)	0.0134
Omentum				
Positive	143	(58)	24 (20–29)	
Negative	92	(37)	24 (10–38)	0.3877
Diaphragm				
Positive	54	(22)	22 (16–29)	
Negative	172	(69)	25 (18–32)	0.1077
Peritoneum (upper abdomen)				
Positive	109	(44)	18 (12–25)	
Negative	131	(53)	29 (24–35)	0.0070
Bone				
Positive	7	(3)	6 (3–9)	
Negative	241	(97)	25 (20–31)	<0.0001
Parametrium				
Positive	28	(11)	18 (11–26)	
Negative	202	(81)	25 (20–30)	0.0338
Postoperative residual disease				
None	62	(25)	48 (27–69)	
≤1 cm	63	(25)	25 (19–31)	
>1 cm	123	(50)	17 (11–22)	0.0004
Intra-abdominal residual disease				
None	101	(41)	48 (30–66)	
≤1 cm	52	(21)	23 (18–27)	
>1 cm	95	(38)	14 (10–19)	<0.0001
Extra-abdominal residual disease				
None	168	(67)	26 (21–31)	
≤1 cm	24	(10)	38 (0–100)	
>1 cm	56	(23)	21 (8–34)	0.3553
Adjuvant therapy				
Yes	220	(89)	26 (21–31)	
No	28	(11)	6 (4–9)	<0.0001
Type of adjuvant therapy				
CT alone	185	(75)	27 (22–32)	
RT alone	11	(4)	12 (0–50)	
CT + RT	24	(10)	26 (4–48)	0.9816
Chemotherapy regimen				
Taxane + platinum	115	(46)	30 (23–37)	
AP ± α	79	(32)	27 (20–34)	
Other	15	(6)	8 (0–16)	0.0470

Univariate analyses

Univariate analyses were performed to identify relationships between OS and demographic, clinicopathological, surgical, and therapeutic variables (Table 4). Of the demographic and clinicopathological variables, PS, histology/grade, myometrial invasion, and LVSI were significantly associated with OS. Fig. 1 shows OS curves according to PS, histology/grade, and adjuvant therapy. Median OS was 79 months in patients with EMG1, 48 months in EMG2, and 14 months in EMG3 + non-EM ($p<0.0001$).

Metastases to para-aortic lymph nodes, pelvic lymph nodes, upper abdominal peritoneum/mesentery, bone, and parametrial invasion were inversely related to OS. The median OS according to stage IVb disease site was 30 months in patients with extra-abdominal metastases alone (n = 57) and 24 months with intra-abdominal metastases alone (n = 155). In the 155 patients with intra-abdominal metastases alone, the median OS was 42 months (95% CI, 0–86) in patients with microscopic disease, 24 months (95% CI, 16–33) with ≤2 cm disease, and 20 months (95% CI, 14–27) with >2 cm disease. This was not significantly different among groups ($p = 0.1527$).

Residual disease showed a significant association with OS ($p = 0.0004$). In patients with intra-abdominal residual disease, smaller size of residual disease was associated with longer OS. In contrast, extra-abdominal residual disease was not related to OS. Median OS was 48 months in patients with no gross intra-abdominal residual disease, 23 months with ≤1 cm residual disease, and 14 months with >1 cm residual disease ($p<0.0001$) (Fig. 2A).

Further stratification according to the presence of extra-abdominal metastases showed that patients with no gross intra-abdominal residual disease survived significantly longer than patients with intra-abdominal residual disease, with or without extra-abdominal metastases (Fig. 2B).

Furthermore, stratification by histology/grade showed a survival advantage in patients who underwent cytoreduction of intra-abdominal disease. Among patients with EMG1/EMG2 type, those with no residual intra-abdominal disease had a longer median OS than those with gross residual intra-abdominal disease (79 vs. 36 months, $p = 0.0226$). The results were similar among patients with EMG3/non-EM type (24 vs. 13 months, $p = 0.0022$).

OS was significantly longer in patients who received postoperative adjuvant chemotherapy and/or radiotherapy than patients who did not receive adjuvant therapy (Fig. 1C). In patients who received postoperative chemotherapy, there was no difference in OS between those who received taxanes plus platinum and those who received AP ($p = 0.5658$).

Multivariate analysis

Cox multivariate analysis was used to simultaneously examine the independent effects on OS of age, PS, histology/grade, myometrial invasion, parametrial invasion, para-aortic lymph node metastasis, pelvic lymph node metastasis, upper abdominal peritoneal/mesenteric metastasis, adjuvant therapy, and intra-abdominal residual disease. Bone metastasis showed a strong correlation with poor prognosis by univariate analysis, but was excluded from the multivariate analysis because there were only 7 patients in this group. The results showed that PS, histology/grade, adjuvant therapy, and intra-abdominal residual disease were independent prognostic factors for OS. The significance of these

Notes to Table 4:
ECOG, Eastern Cooperative Oncology Group; LVSI, lymphovascular space invasion; AP ± α, doxorubicin + platinum ± ifosfamide/cyclophosphamide/5FU/VP16; CT, chemotherapy; RT, radiotherapy.
[a] Numbers may not add up to the total because some data are unknown.
[b] Patients with unknown status were excluded from the calculation of log-rank p-values.

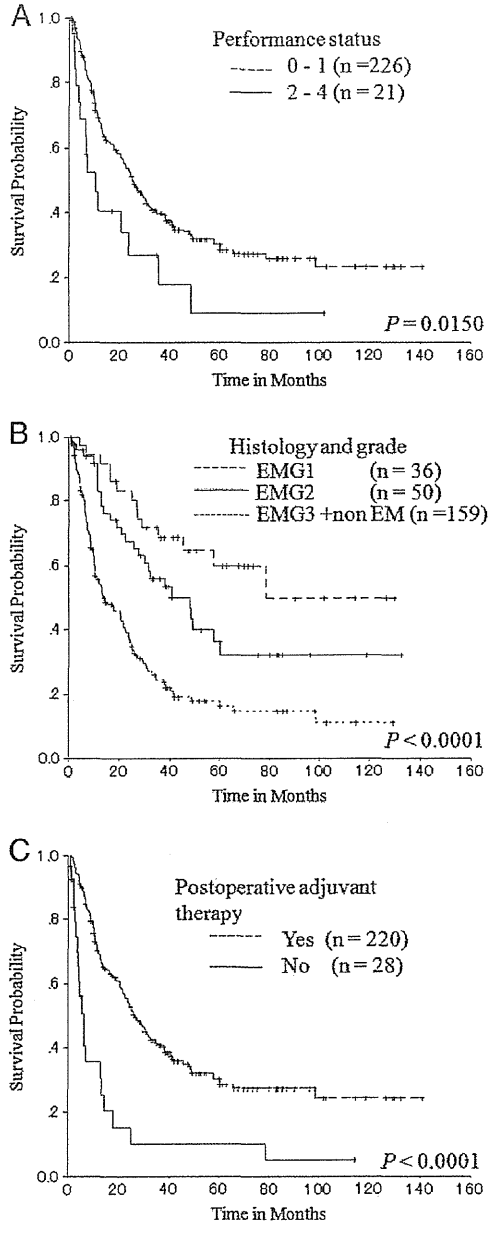

Fig. 1. Kaplan–Meier curves for overall survival (OS). A: Median OS time according to performance status (PS): PS 0–1(dashed line), 25 months; PS2–4 (solid line), 11 months. B: Median OS time according to histology/grade: endometrioid (EM) grade 1 (dashed line), 79 months; EM grade 2 (solid line), 48 months; EM grade 3 + non-EM (dotted line), 14 months. C: Median OS time according to adjuvant therapy: yes (dashed line), 26 months; no (solid line), 6 months.

variables was as follows: PS (0–1 vs. 2–4) (hazard ratio [HR] = 1.988; 95% CI, 1.108–3.569; $p = 0.021$), histology/grade (EMG1 vs. EMG2 vs. EMG3 + non EM) (HR = 2.245; 95% CI, 1.652–3.050; $p < 0.001$), adjuvant therapy (yes vs. no) (HR = 3.396; 95% CI, 1.898–6.076; $p < 0.001$), and intra-abdominal residual disease (none vs. ≤1 cm vs. >1 cm) (HR = 1.499; 95% CI, 1.203–1.867; $p < 0.001$).

Discussion

Our study is the largest retrospective series exploring the clinical outcome of surgical stage IVb EMCA, including patients with extra-abdominal metastases. Our study also investigated the clinicopathological variables of these patients.

Although surgical staging is the most basic treatment for EMCA [1,2], intra-abdominal metastases are poorly recognized without staging laparotomy. Although several reports have documented disease distribution in surgical stage IVb patients, the reports lacked detailed information, or did not classify patients according to intra- or extra-abdominal disease. Bristow et al. reported that the most common intra-abdominal metastatic sites were the pelvis, peritoneum, omentum, and retroperitoneal nodes [7]. The distribution of metastatic disease sites in our study was comparable with previously reported distributions. In the present study, 77% of surgical stage IVb patients had upper intra-abdominal disease, and 78% had intra-pelvic spread and/or retroperitoneal lymph node metastases. However, most upper intra-abdominal disease was not detected by preoperative imaging studies. Goff et al. reported that preoperatively unrecognized upper intra-abdominal disease occurred in 53% of surgical stage IV patients [8]. In our study, the size of intra-abdominal stage IVb disease was ≤2 cm in half of the patients, which seemed to be smaller than the disseminated disease found in cases of advanced ovarian cancer. This may be one of the reasons why preoperative diagnosis is difficult. Metastasis to the diaphragm was documented in 22% of patients in the present study. This may be valuable information for gynecologic oncologists. The importance of thorough observation of the entire abdominal cavity, including the diaphragm, is stressed.

Few reports of stage IVb EMCA patients have discussed the relationship between survival and histological factors, which is known to be significant in stage I–III patients [1,2]. This is the first study to report a detailed evaluation of histopathological factors in stage IVb EMCA. As the unfavorable histopathological factors such as serous subtype or LVSI have a higher propensity for extrauterine metastasis, patients with these factors are more likely to present with advanced-stage disease. Most patients in the present study had these factors. Univariate analyses showed that non-endometrioid type, high-grade endometrioid type, deep myometrial invasion, and positive LVSI were significantly associated with poor prognosis. Multivariate analysis showed that histology/grade was an independent prognostic factor. Patients with lower-grade endometrioid type are expected to have a longer survival time, even in stage IVb EMCA.

The favorable impact of surgical cytoreduction on survival has been well demonstrated in advanced ovarian cancer [15,16]. Greer and Hamberger first suggested the beneficial effect of cytoreductive surgery and postoperative radiotherapy in advanced EMCA [17]. Subsequently, several reports on advanced EMCA have demonstrated improved OS in patients who undergo optimal cytoreductive surgery, including all histological subtypes [4,7–9,18], endometrioid subtype [10], and serous subtype [11,12,19]. Barlin et al. performed a meta-analysis of 14 retrospective cohort studies including 672 patients with advanced or recurrent EMCA who underwent cytoreductive surgery [13]. Although primary stage IV patients accounted for only 60% of the patients in their analysis, complete cytoreduction to no gross residual disease was associated with superior OS.

Generally, distant metastases are considered to be a poor prognostic factor. The association between extra-abdominal metastases and prognosis has not previously been discussed, because studies have included few patients in this group. In our study, the frequency of extra-abdominal metastases was 38%, which is the highest reported frequency compared with previous reports of surgical stage IVb EMCA. Ayhan et al. reported that the prognosis of patients with extra-abdominal metastases was poor [4]. Bristow et al. reported that optimal debulking was not achieved in patients with extra-abdominal metastases [7]. Most extra-abdominal metastases are unresectable, and in our study complete resection of extra-abdominal metastases was achieved in 13 patients (14%). It is unclear whether laparotomy benefits patients with unresectable extra-abdominal metastases. Recently, Ueda et al. reported a small study which demonstrated that optimal cytoreduction was associated with improved survival even in stage IVb EMCA patients with extra-abdominal metastases [6].

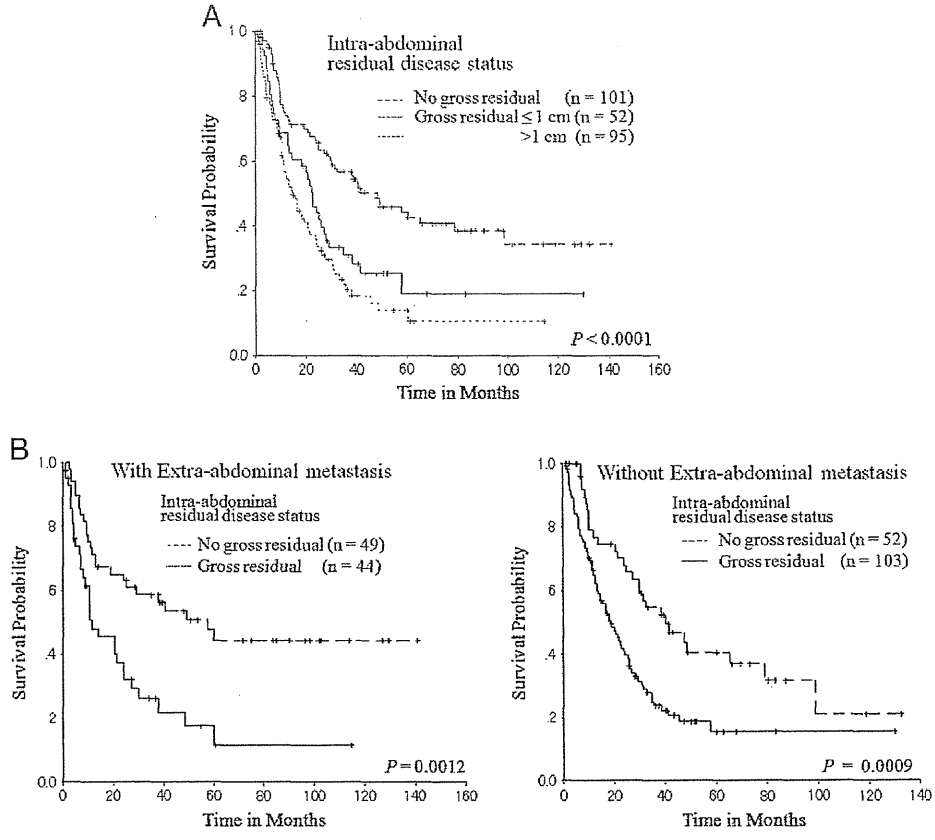

Fig. 2. Kaplan–Meier curves for OS. A: Median OS time according to intra-abdominal residual disease: no residual disease (dashed line), 48 months; ≤1 cm residual disease (solid line), 23 months; >1 cm residual disease (dotted line), 14 months. B: Median OS time according to intra-abdominal residual disease in patients with (left) and without (right) extra-abdominal metastases. (left): no residual disease (dashed line), 58 months; gross residual disease (solid line), 11 months. (right): no residual disease (dashed line), 40 months; gross residual disease (solid line), 18 months.

The distribution of extra-abdominal disease in this cohort is not identical to that of all stage IVb patients because selection bias for surgery is expected. The majority of patients with extra-abdominal metastases in this cohort had metastases involving only one anatomical region, a good PS, and no symptoms. This group of patients may therefore have had less aggressive disease or a better response to adjuvant chemotherapy than patients with extra-abdominal metastases who did not undergo surgery. We were unable to definitively determine which characteristics were good prognostic factors in patients with extra-abdominal metastases. However, extra-abdominal disease was not associated with poor prognosis in this study. The OS was significantly longer in patients who underwent intra-abdominal cytoreduction than in patients with remaining gross intra-abdominal disease, even in patients with extra-abdominal metastases. We suggest that aggressive surgery should be undertaken to achieve complete macroscopic resection of all intra-abdominal disease if the patient's general condition is good.

The Gynecologic Oncology Group reported that systemic postoperative adjuvant chemotherapy with cisplatin + doxorubicin was associated with improved survival compared with postoperative whole abdominal irradiation [20]. Therapy with paclitaxel + doxorubicin + cisplatin was reported to be superior to doxorubicin + cisplatin [21]. In patients with advanced EMCA, platinum + anthracyclines and taxanes seem to be the most promising agents. Some prospective and retrospective studies of combination adjuvant chemotherapy and radiation for advanced or recurrent EMCA have been conducted [22–24]. However, no studies have focused on adjuvant treatment of stage IVb EMCA.

In the present study, adjuvant therapy was associated with longer OS. Most patients received chemotherapy alone as postoperative treatment, including taxanes + platinum or AP. There were no differences in OS between these two treatment groups. Although it is certain that chemotherapy is an ideal treatment for this systemic disease, we cannot comment on treatment outcomes according to the type of postoperative therapy due to the heterogeneity of treatment schedules in our cohort.

This study has several limitations. First, because it was a retrospective multicenter study, the quality of data may not be uniform. We made a considerable effort to collect uniform data using a case report form to standardize the information collected as much as possible. Second, there were heterogeneous treatment protocols in different institutions. In particular, there may have been a selection bias for the type of treatment initially chosen in patients with distant metastases. Third, the question of whether the improved outcome of patients who undergo optimal cytoreduction is due to the surgery or to the biology and aggressiveness of the tumor is unresolved.

In conclusion, our retrospective study showed that PS, histology/grade, postoperative treatment, and intra-abdominal residual disease were independent predictors of survival in patients with stage IVb EMCA who underwent primary cytoreductive surgery. Cytoreductive surgery and postoperative therapy may prolong survival time in some patients with stage IVb EMCA, particularly those with relatively favorable prognostic factors, even in the presence of extra-abdominal metastases.

Conflict of interest statement

The authors have no conflicts of interest.